Sea ice conditions from Synthetic Aperture Radar data

Prof. Stein Sandven
Nansen Environmental and Remote Sensing Center
and
UNIS

Contents

- Sea ice processes, dynamic and thermodynamic
- Observing sea ice with satellite remote sensing
- Synthetic Aperture Radar (SAR)
- Sentinel-1: a new era of vast production of open data
- Properties of radar systems
- Microwave interaction with sea ice
- Example of SAR sea ice observations
- Algorithms to retrieve sea ice variables
- Evolution of SAR data usage

Sea ice processes - thermodynamic

Melt/freeze – sum of all energy fluxes affecting the ice, strong impact of snow

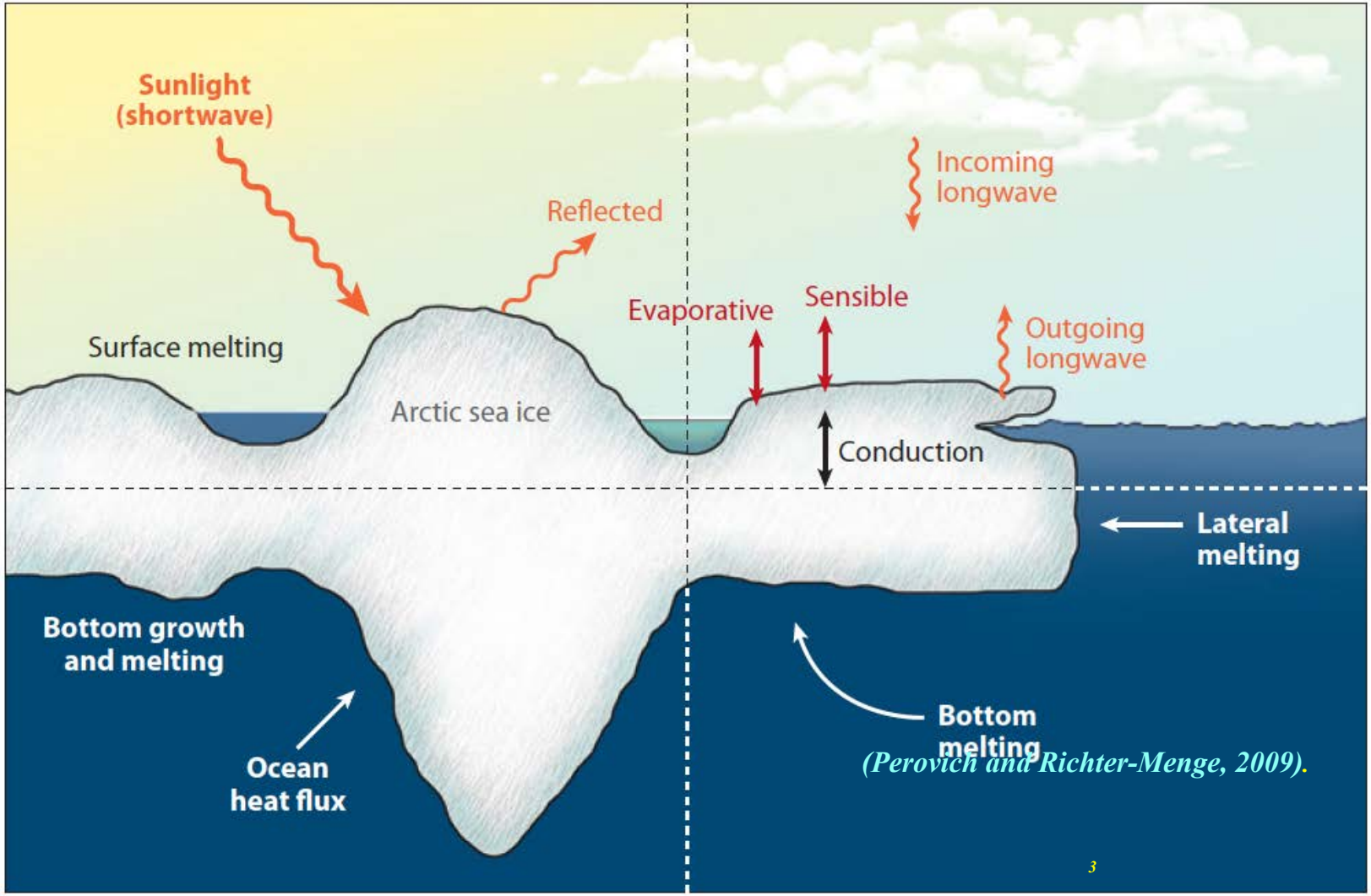

Sea ice processes - dynamic

Coastal area

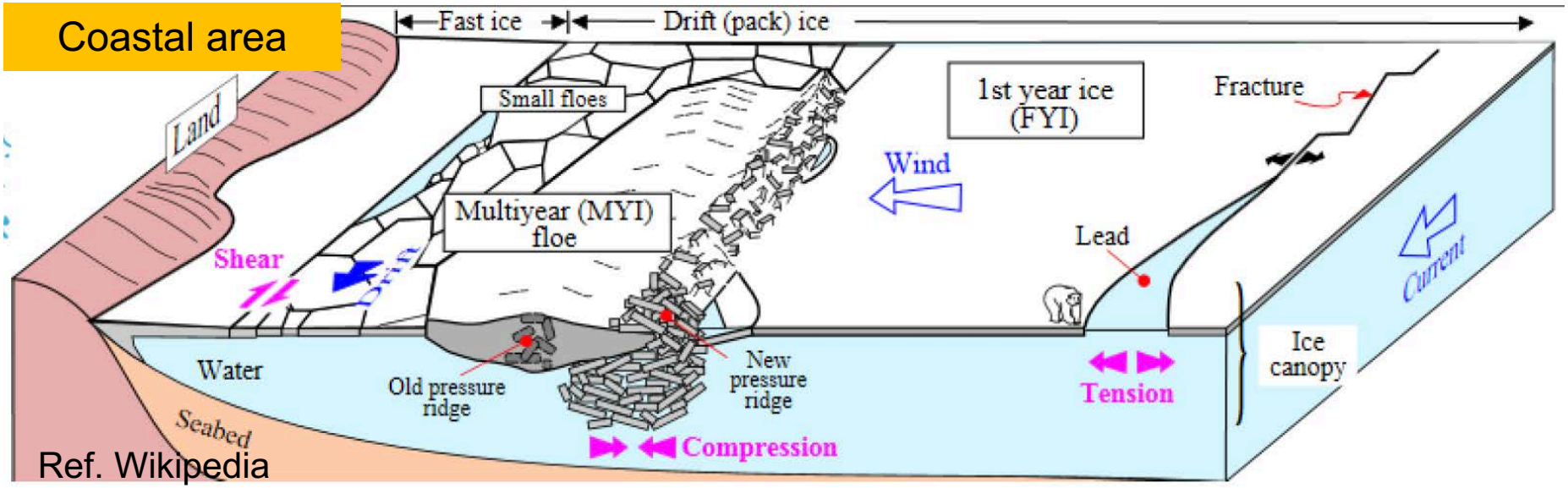

Ref. Wikipedia

Open ocean

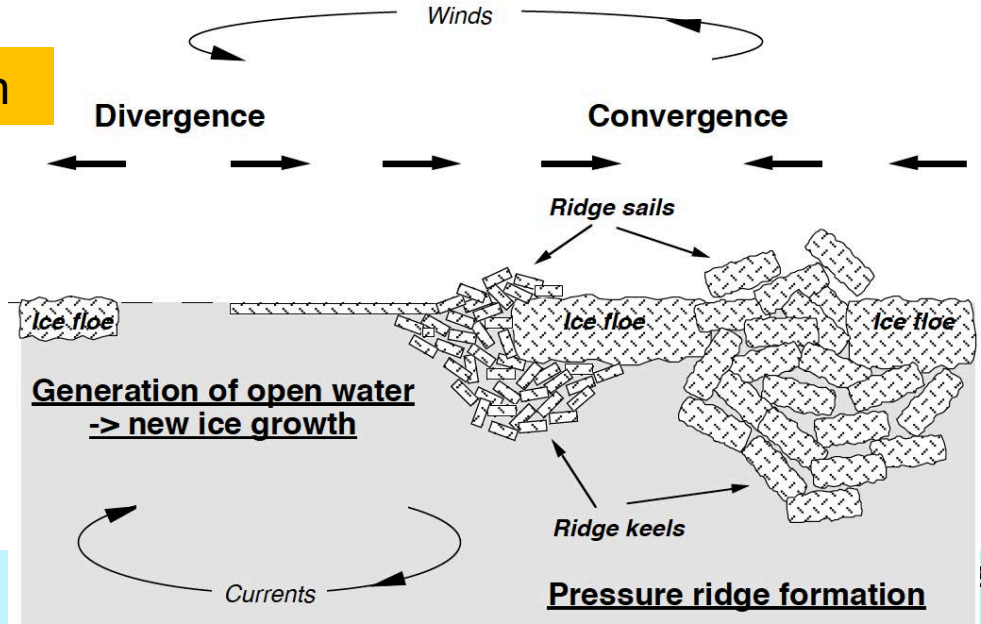

All motion-related processes: forced by wind, currents, waves, internal ice stress

Ref. C. Haas

Ridging and rafting

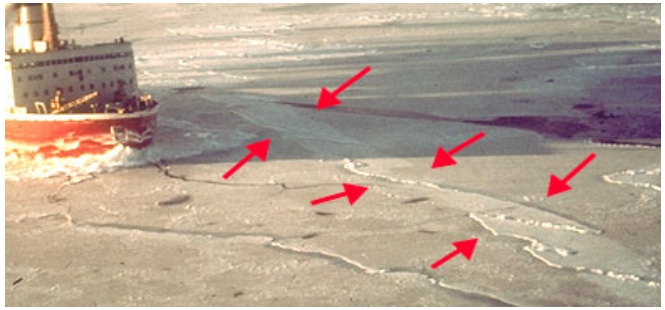

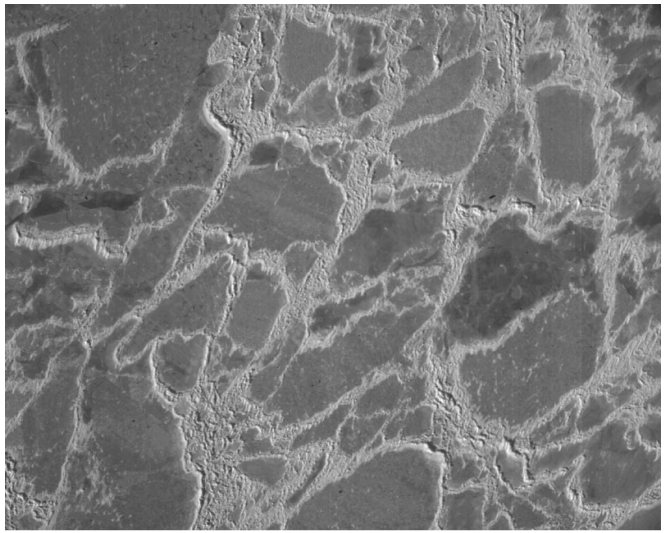

Vertical video picture from helicopter: about 1 x 1 km

Ridging and rafting occurs in sea ice when winds, currents or internal ice stress generate convergence in the ice field. The largest ridges often occur near land or islands where sea ice is piled up at the shallow sea floor. The spatial distribution of ridges compared to undeformed ice is shown in the vertical video picture to the left. Typical height of ridges is from 0.5 - 2.0 m. Extreme ridge heights of more that 10 m can occur when ice is pushed against a shore or is grounded in shallow water.

Convergene of thick ice (> 1 m) results in ridge formation

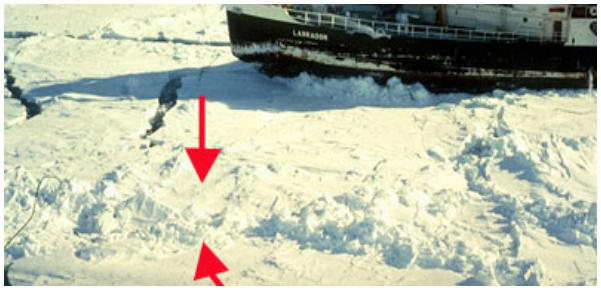

Wave-ice interaction - dominant in the marginal Ice Zone

Formation

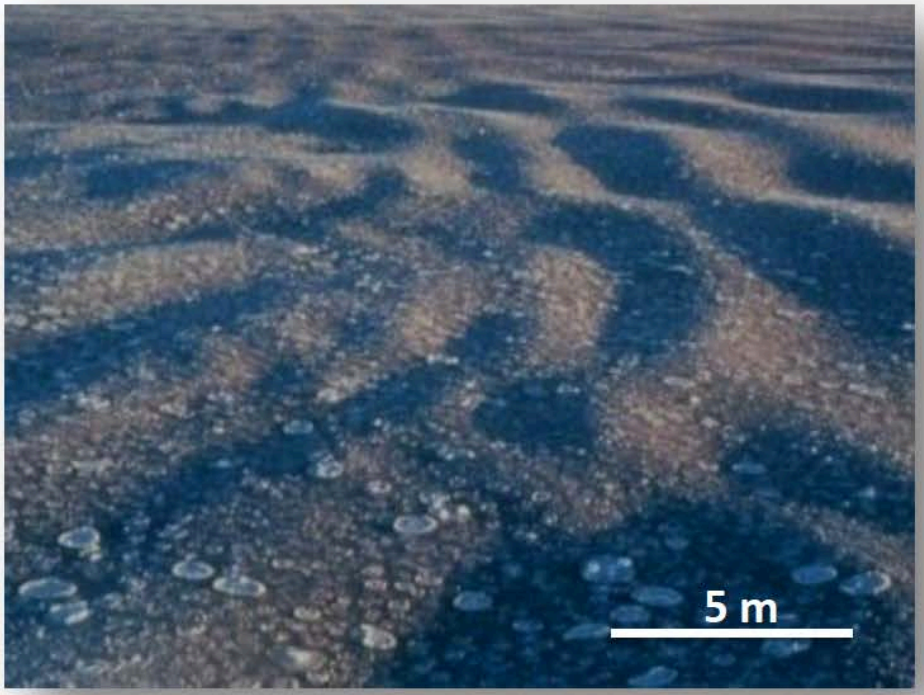

Breakup / destruction

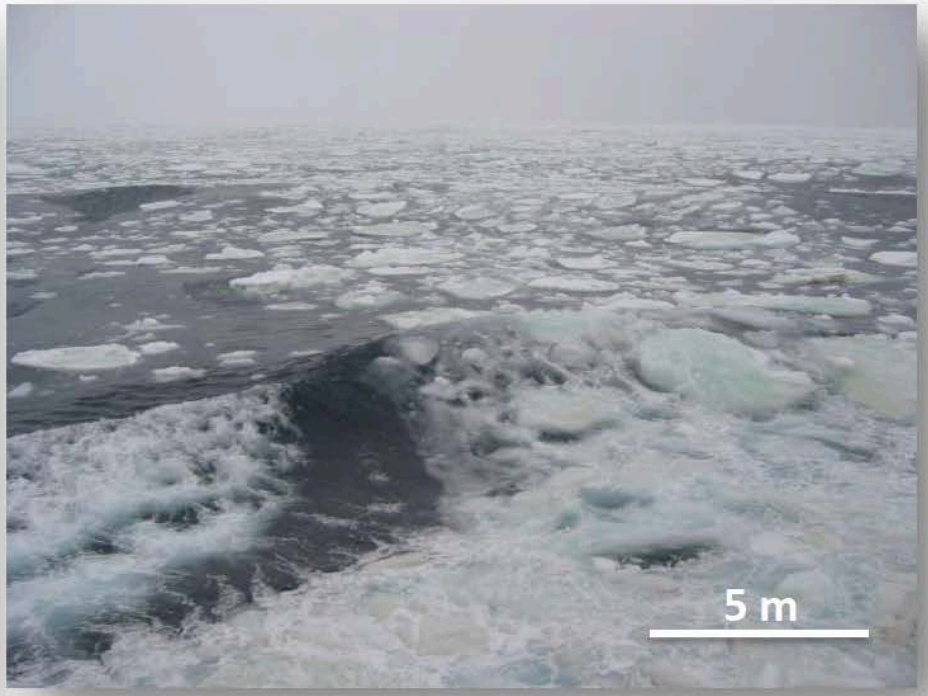

Ref. Massom , 2017

Sea ice types during freezing

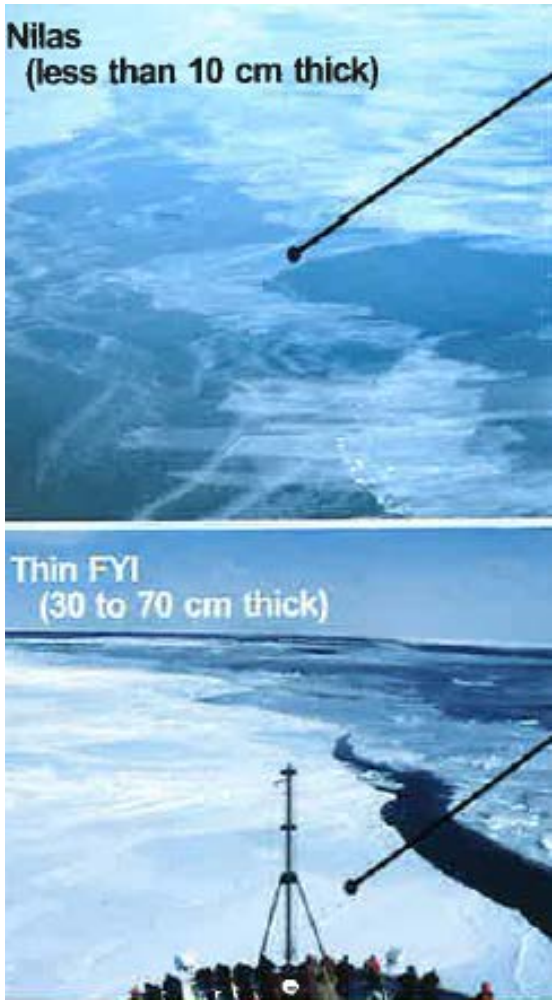

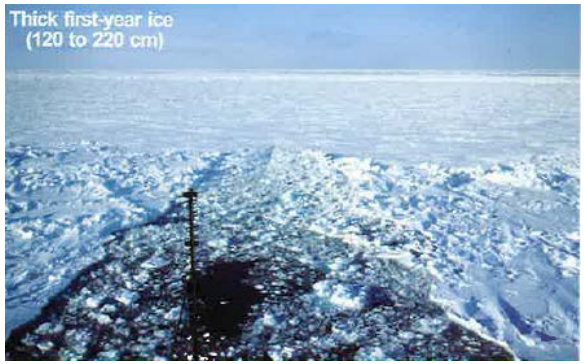

Ref. M. Johnson

Sea ice melting

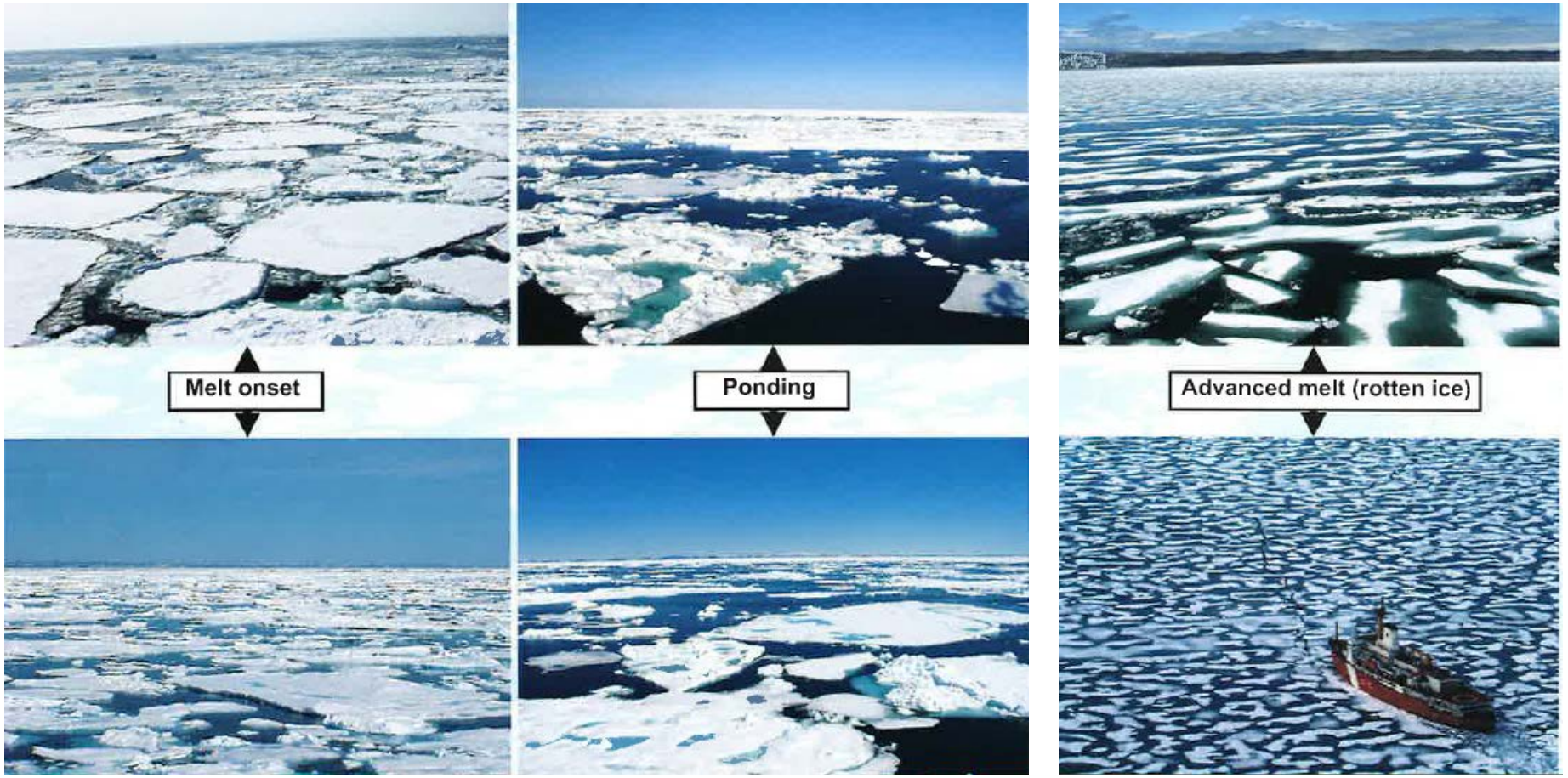

Ref. M. Johnson

Observing sea ice parameters by satellite sensors

Ice variable	Remote sensing data	Research and operational status
Area, extent and concentration	Passive microwave data Scatterometer data Visual/IR data	Global products are available daily from SSMI, AMSR-E, and scatterometer data Operational ice charts are produced with support form visual and IR data
Ice thickness	Radar altimeter / Laser altimeter	Large-scale maps for the Arctic have been demonstrated by ERS data. Expected products from CRYOSAT from 2010
	L-band passive microwave data	SMOS data from 2010, thin ice thickness
	IR data using thermodynamic equation	AVHRR, MODIS, etc, during late winter, spring, thin ice thickness
Ice drift	Passive microwave data Scatterometer data SAR wideswath data	Operational products are available using scatterometer and passive microwave data SAR-based ice drift is available for selected regions and periods
Ice-snow albedo, melt ponds, surface temperature, etc.	Optical / IR images	Research activity, pathfinder data sets have been produced
Ice type classification / ice age	Scatterometer, SAR and passive microwave	Multi-year and first-year products are available, various levels of young and first-year ice can be produced from SAR
Ice roughness	Radar and laser altimeter, SAR	Research products from Icesat and CryoSat, SAR provides indicators
Icebergs in the Arctic and Antarctic	High resolution optical and SAR images, scatterometer	Monitoring service in some regions

Microwave versus visual/infrared remote sensing of sea ice

Visual and infrared radiometry

- cloud cover inhibits surface observations
- snow cover (high albedo) dominates the signal
- water and wet ice/wet snow reduces the albedo
- sensitive to temperature: thin ice, leads
- not sensitive to other ice properties

Passive microwave radiometry and active radar systems

- independent of cloud and light conditions
- penetrate snow during dry/cold conditions
- sensitive to ice properties:
- salinity, crystal structure, surface roughness
- sensitive to water and moist in snow

Radar bands in the EM spectrum

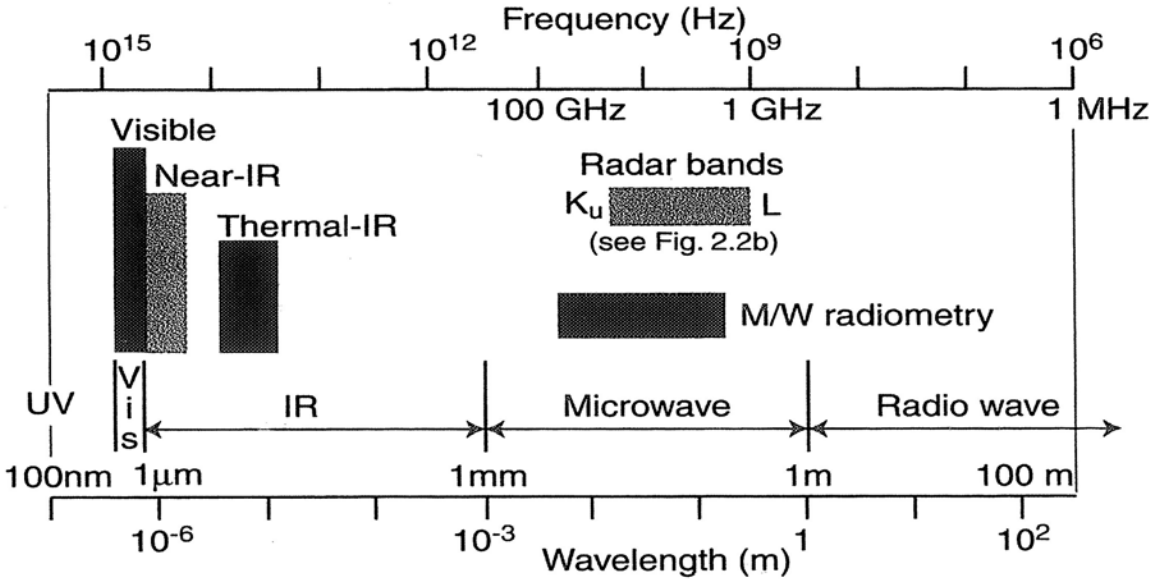

(a)

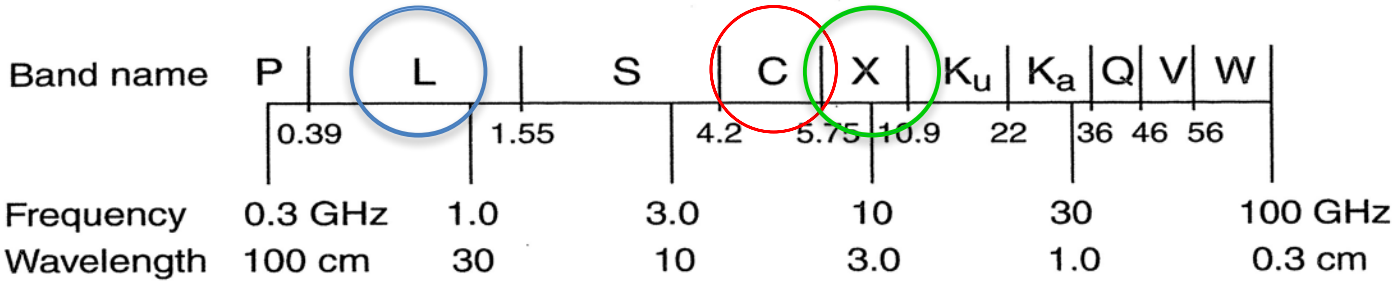

(b)

SAR satellites from 1991

RISAT 2012-2016

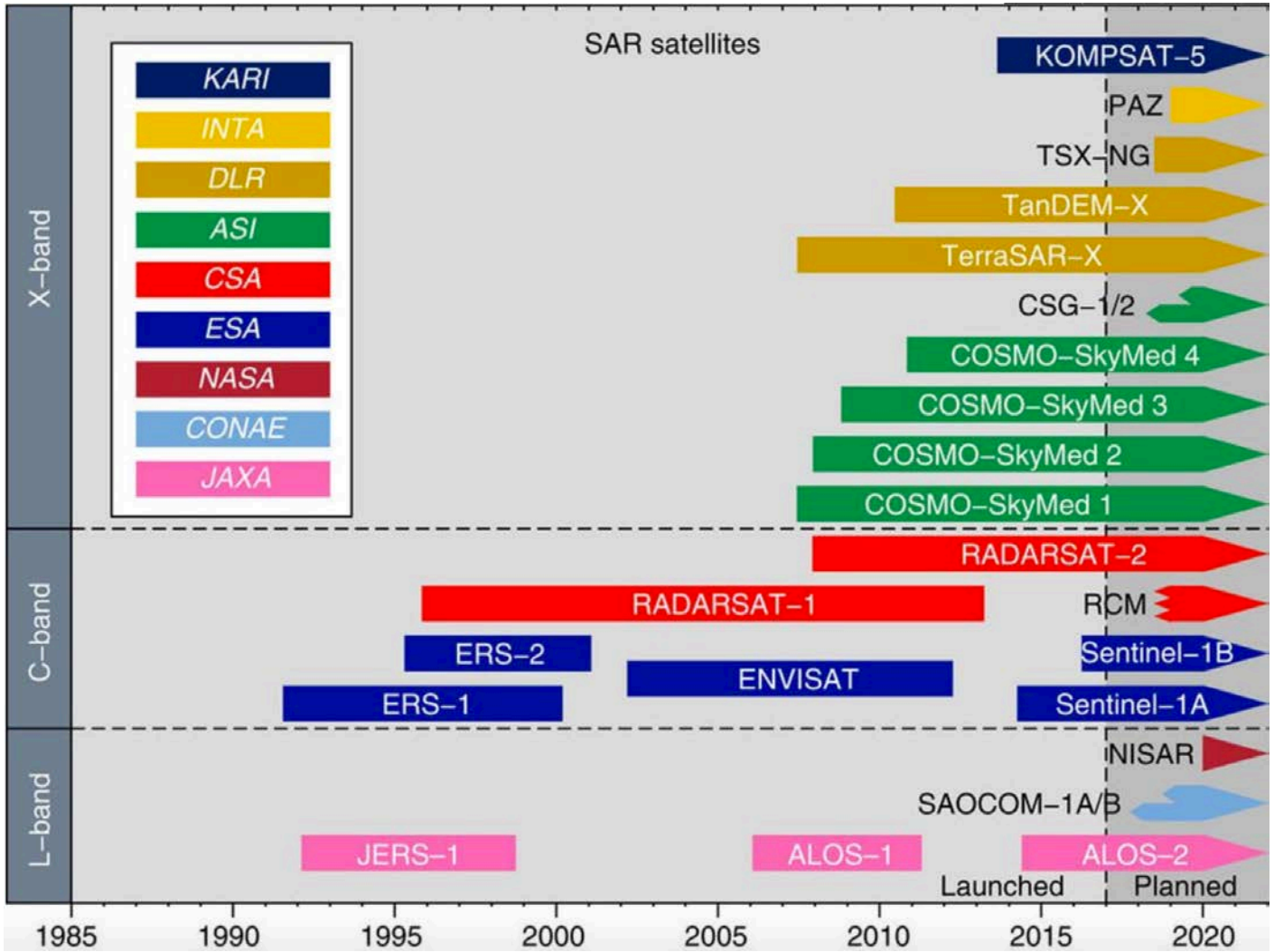

https://www.nature.com/articles/ncomms1384

Sentinel-1 applications

- monitoring sea ice zones and the polar environment
- monitoring of marine environment (wind, waves, fronts, eddies)
- ice sheet and glacier changes
- oil spill detection
- ship detection

Sentinel-1 SAR imaging modes

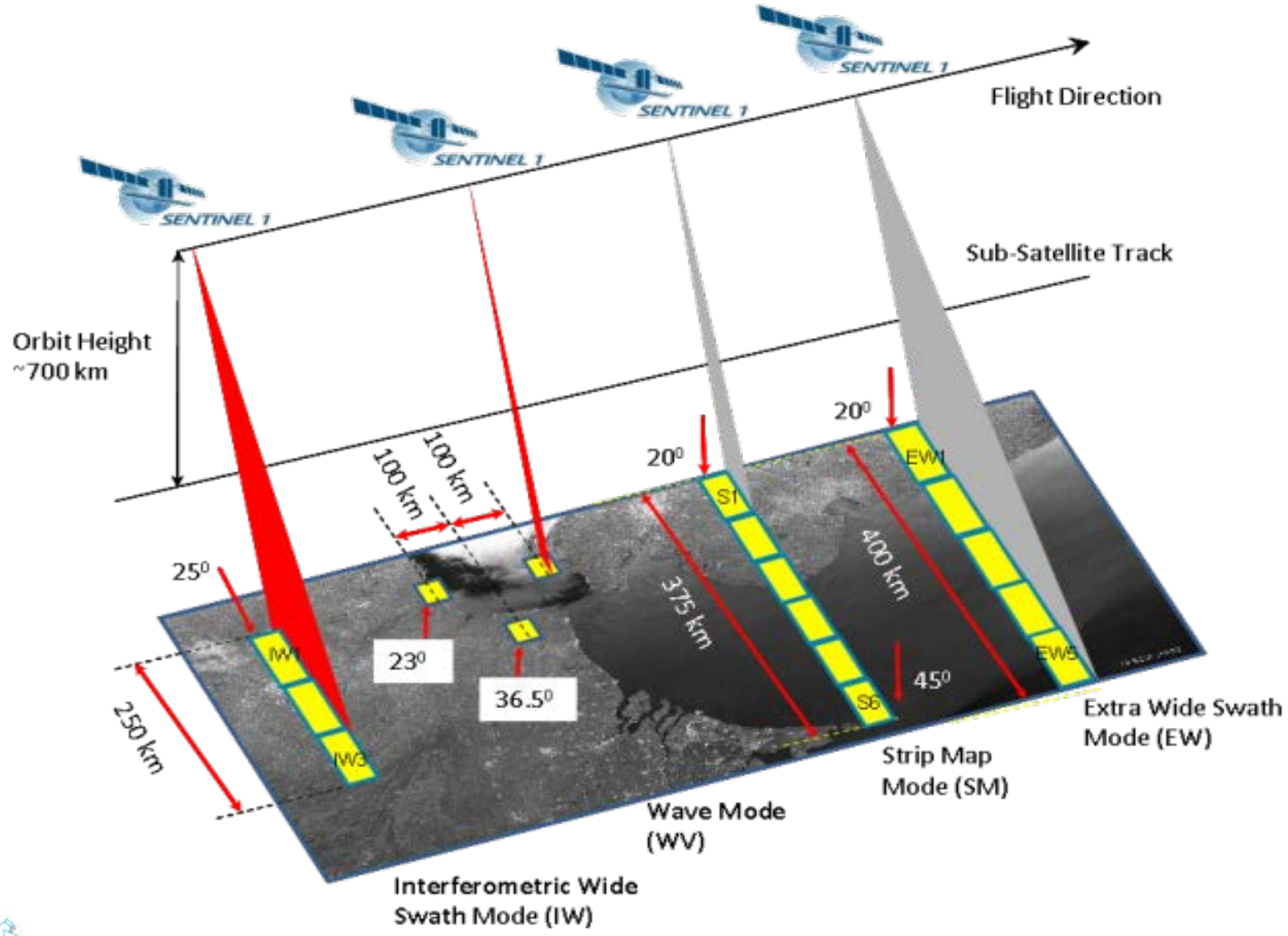

Sentinel-1 Constellation Observation Scenario: Mode - Polarisation - Observation Geometry

sentinel-1

validity start: 02/2018

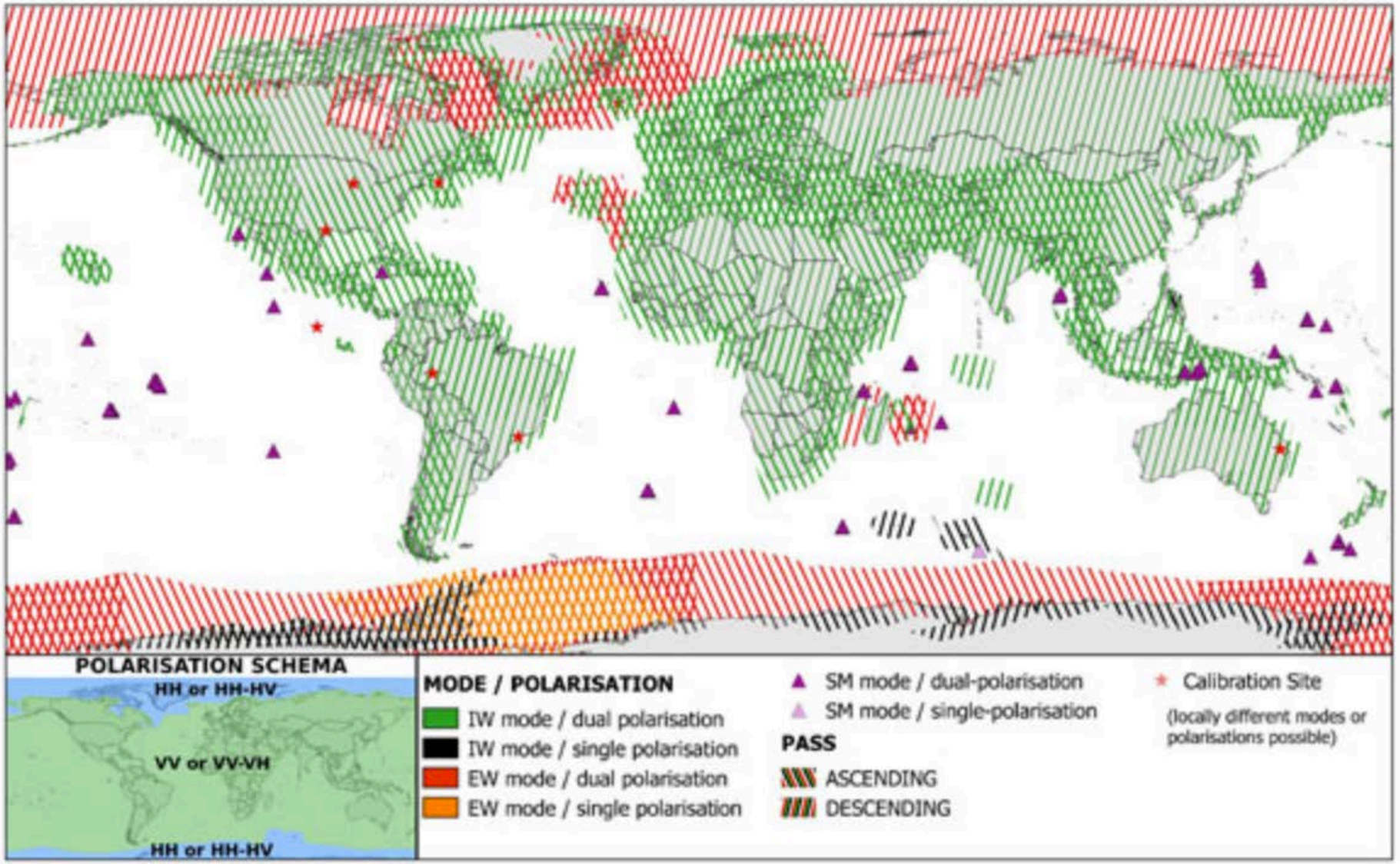

Sentinel-1 SAR image coverage last 72 hours

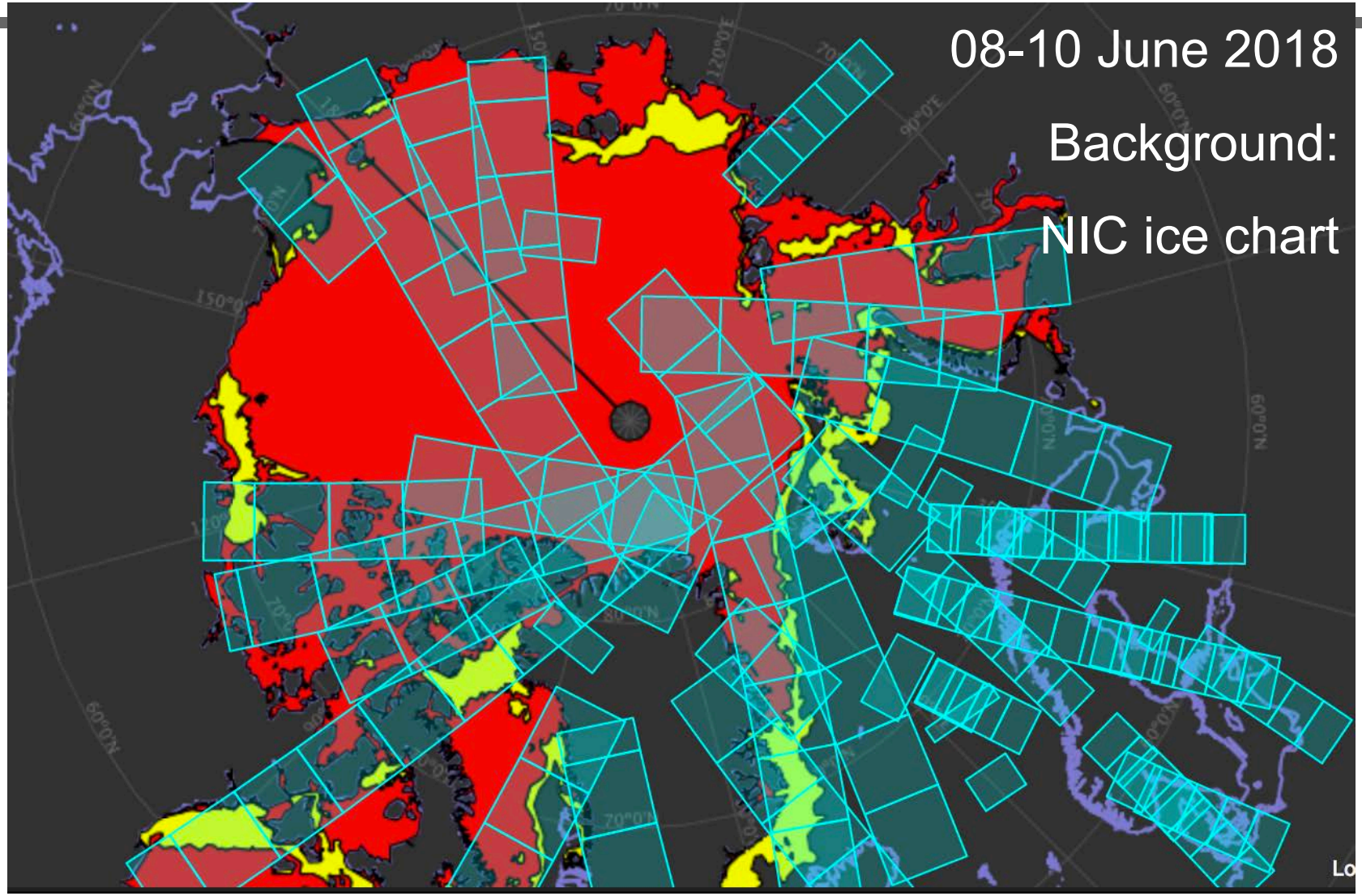

http://www.polarview.aq/arctic

Sentinel-1A/B coverage of the Arctic
09 June 2018 (3-day mosaic)

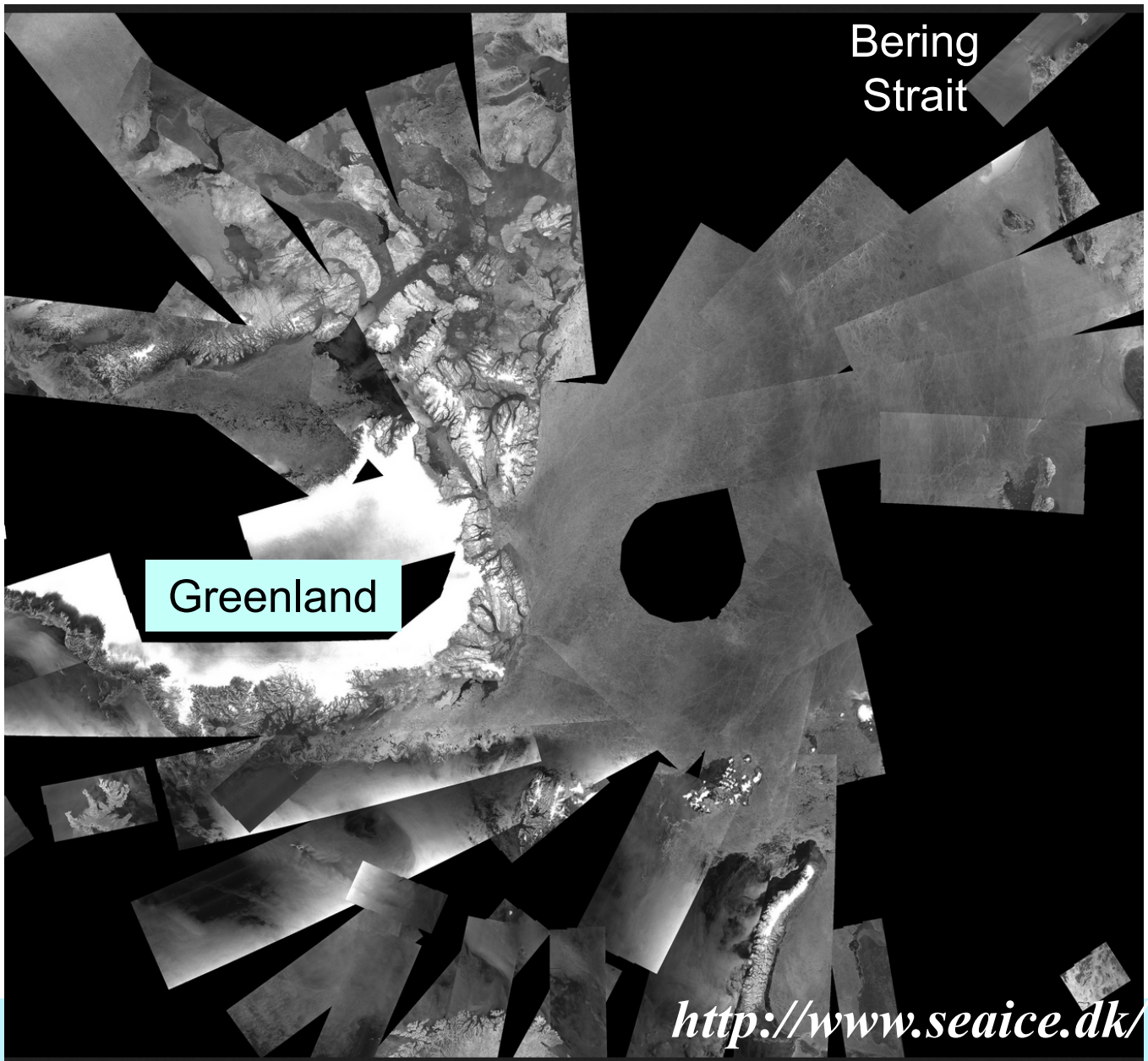

NERSC

Time sequence 01 Jan – 09 Mar 2018

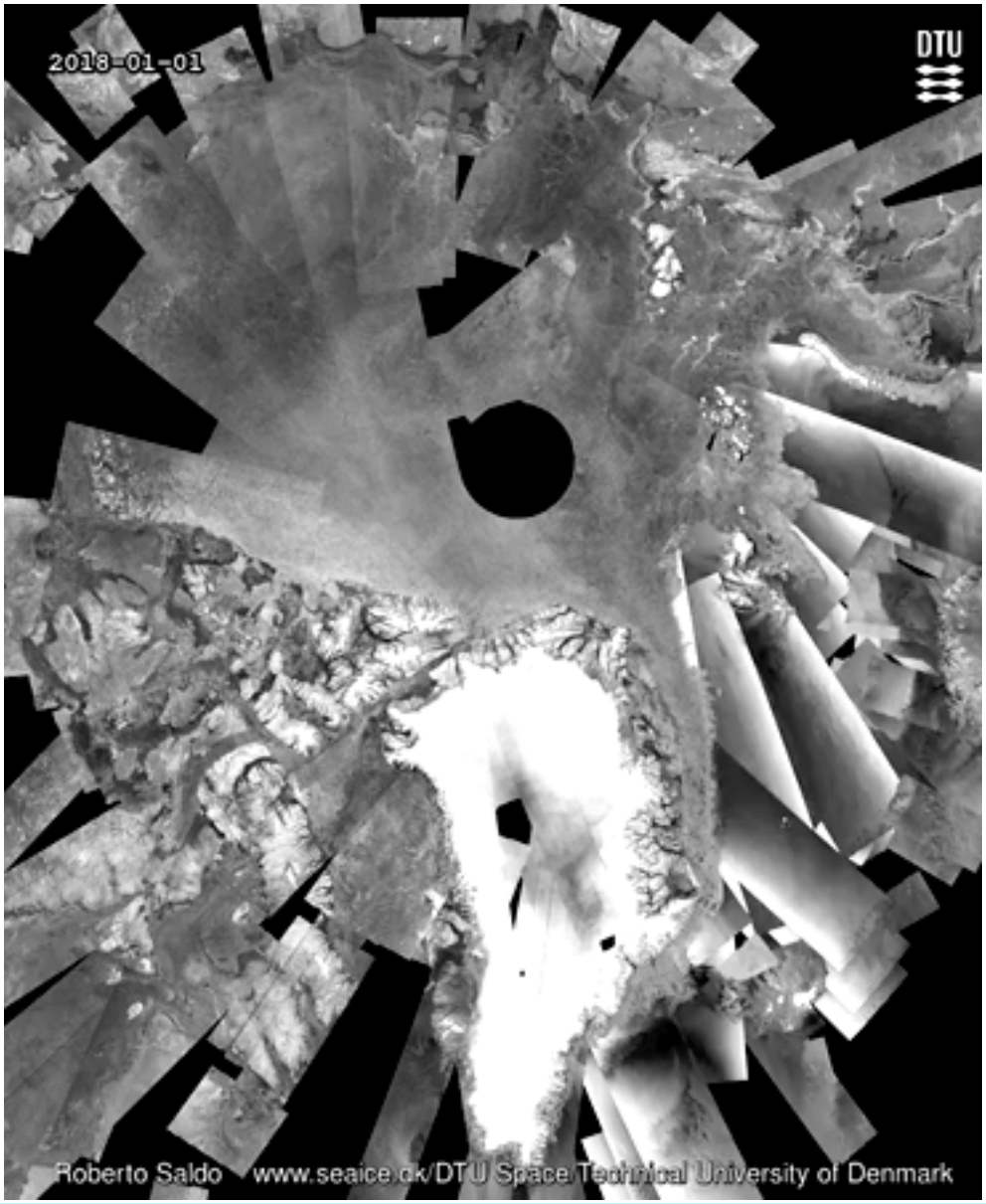

Regular sea ice products from OSI TAC
(Copernicus Ocean and Sea Ice Thematic Assembly Centre)

- Global Sea Ice Concentration, Edge, Type and Drift from EUMETSAT OSI SAF.
- Global Sea Ice Concentration Time Series from EUMETSAT OSI SAF
- Arctic ice drift from IFREMER
- Global high resolution SAR Sea Ice drift from DTU.
- Regional high resolution Sea Ice Charts for the European seas (met.no, FMI, DMI)
- Regional SAR Iceberg Density around Greenland from DMI.
- Regional SAR Sea Ice Type for the Arctic from NERSC.
- Regional SAR Sea Ice Type for the Antarctic from BAS

http://cmems.met.no/SIW-TAC/

Regional ice chart for the European Arctic sector

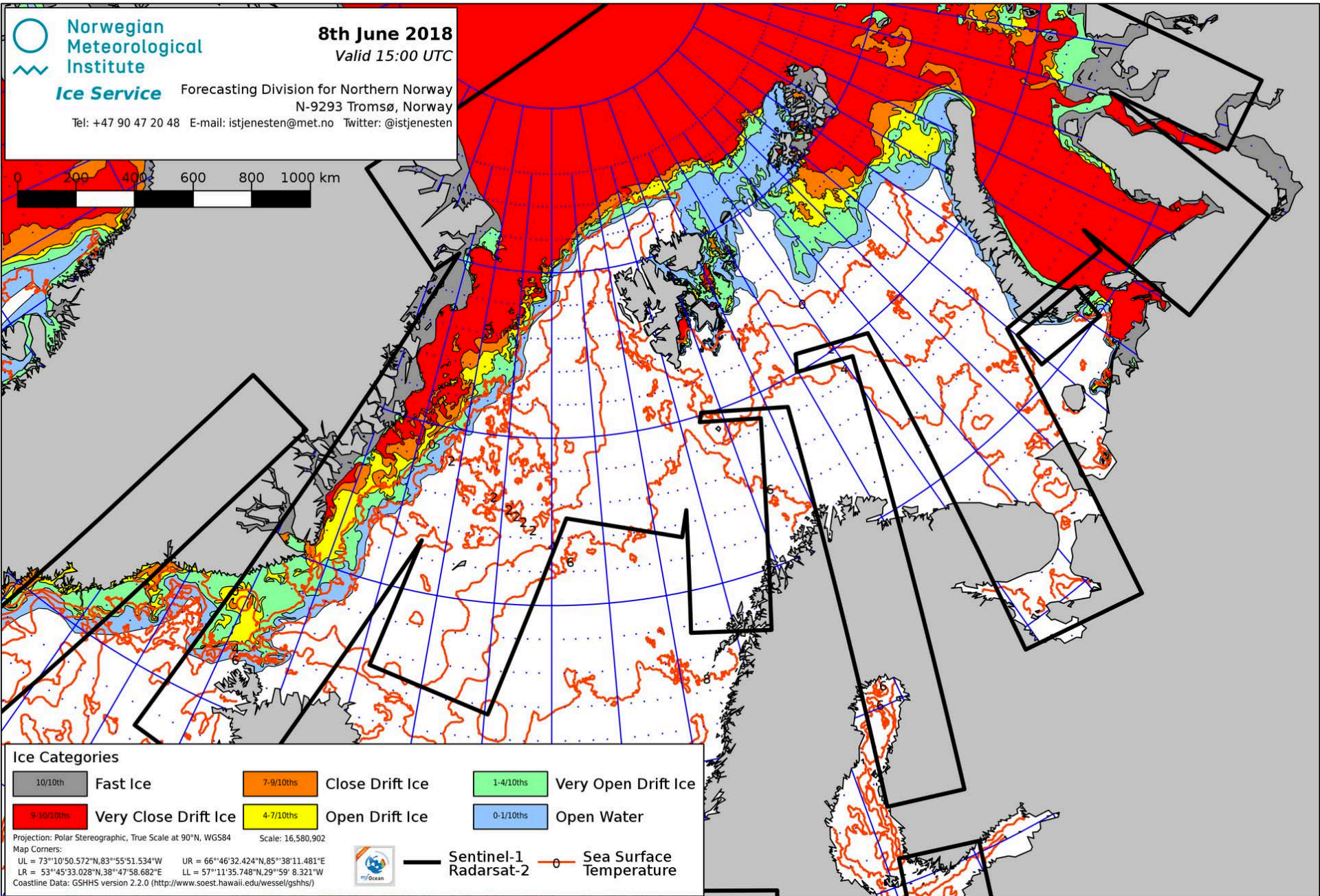

Properties of radar systems

1 radar signals are extremely sensitive to the surface roughness of the area being imaged,

2 radar signals do not detect the visible color of the surface, but detect moisture (or lack of) and electrical properties of the surface,

3 radar systems record the phase and polarization characteristics of the reflected microwave pulse,

4 radar signals produce images with speckle due to the coherent nature of the system,

5 radar signals produce images with certain geometrical distortions, such as slant range geometry, image layover and shadowing, and

6 radar signals are sensitive to motion of objects in the imaged area.

Radar Operation

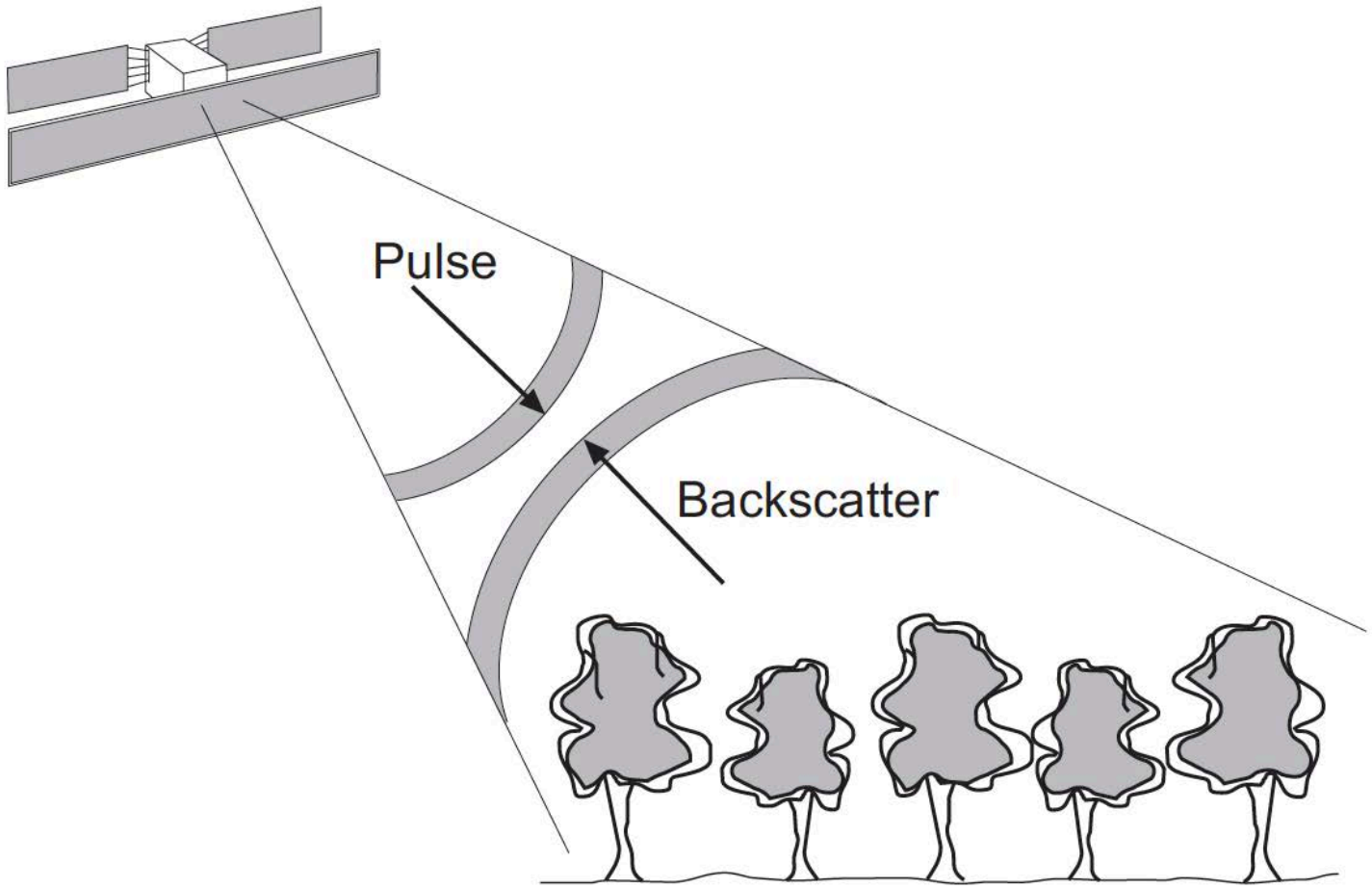

Single Pulse Time - Space Diagram

3

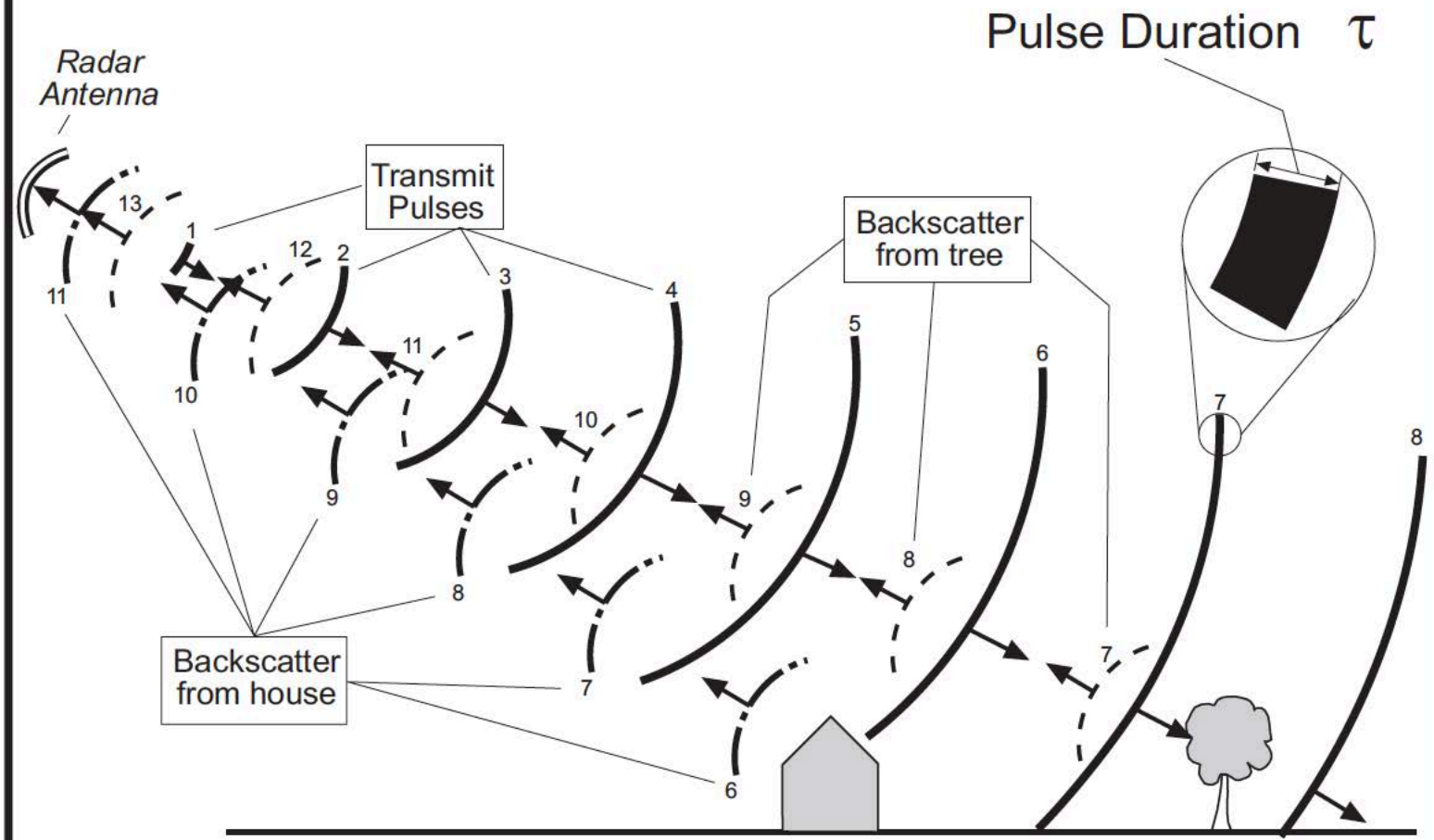

Microwave scattering from sea ice is controlled by

1) The Complex Dielectric Constant (determined by ice type, thickness, salinity, temperature, snow depth, freeze onset date, etc) indicates reflectivity, conductivity, moisture, penetration depth

2) The inhomogeneities of Scattering Inclusions (surface scattering, volume scattering)

3) The Frequency, Polarization and Sensor Geometry of the SAR

Surface scattering

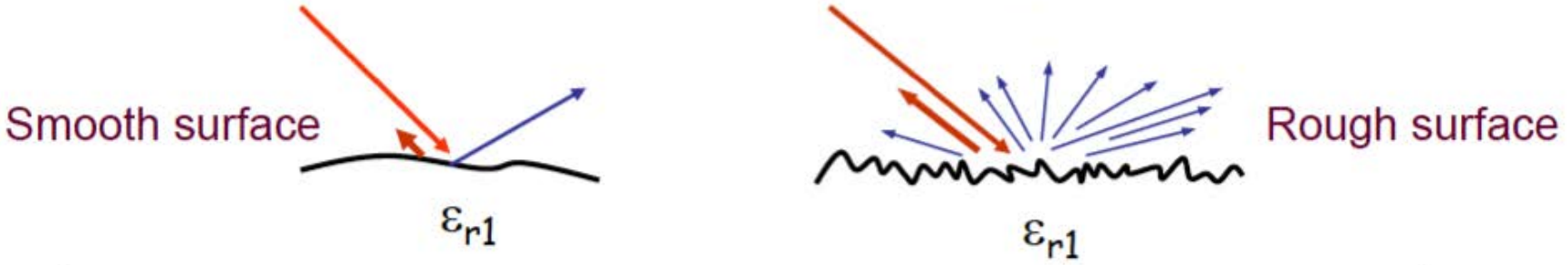

The roughness of the surface (wrt to the wavelength) governs the scattering pattern

$\varepsilon_{r2} > \varepsilon_{r1}$ medium 2 is wetter than medium 1

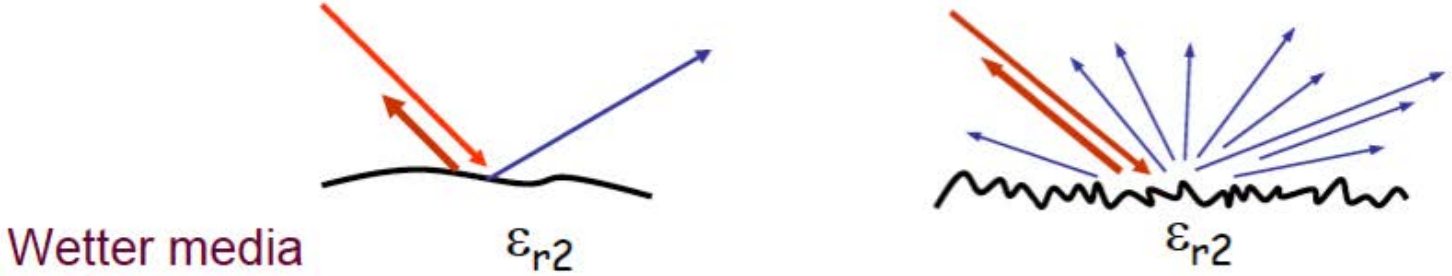

The dielectric constant (moisture content) of the medium governs the strength of the backscatter

- The dielectric constant increases with increasing moisture
- The reflectivity increases with with increasing dielectric constant

Scattering of radar waves from smooth and rough surfaces relative to wavelength

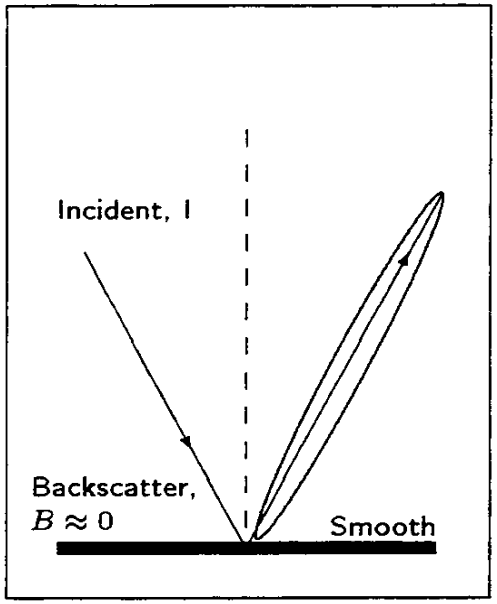

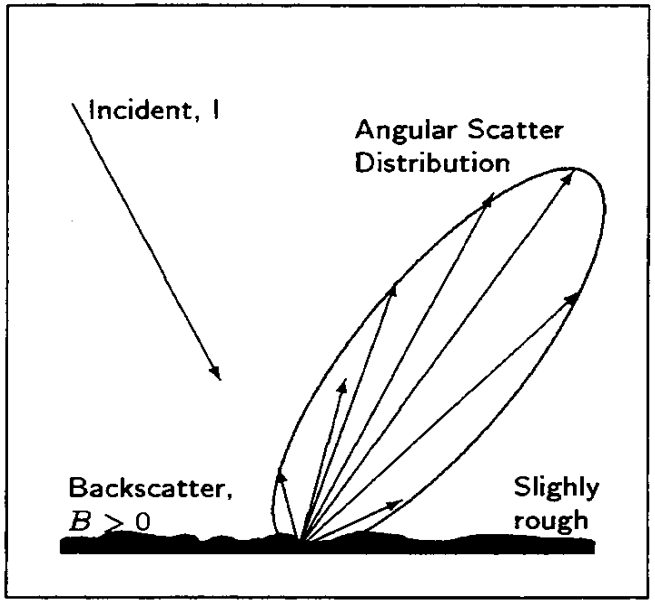

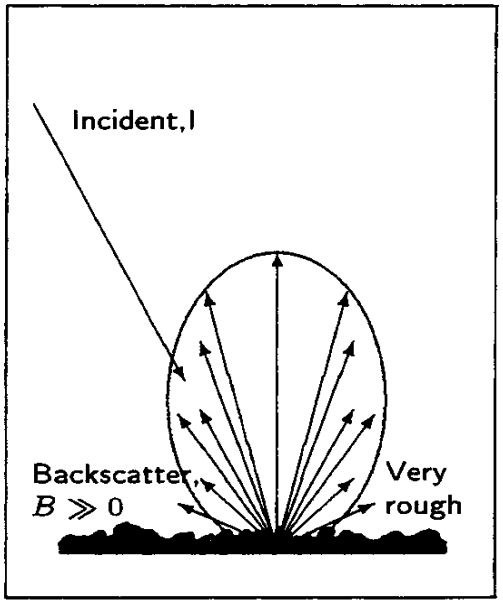

Scattering of radar waves from ice surfaces

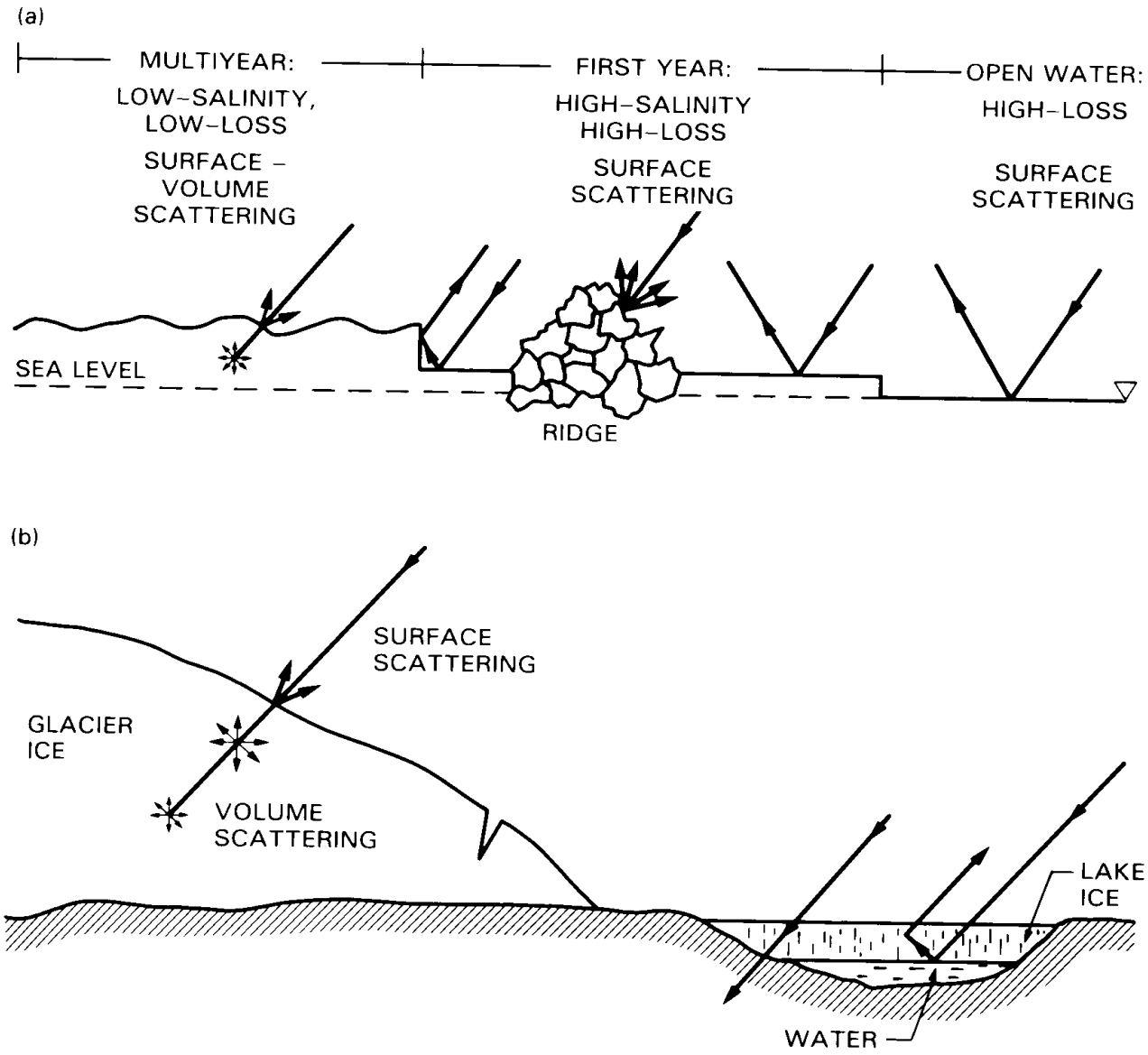

Backscatter from multiyear ice, firstyear ice and open ocean

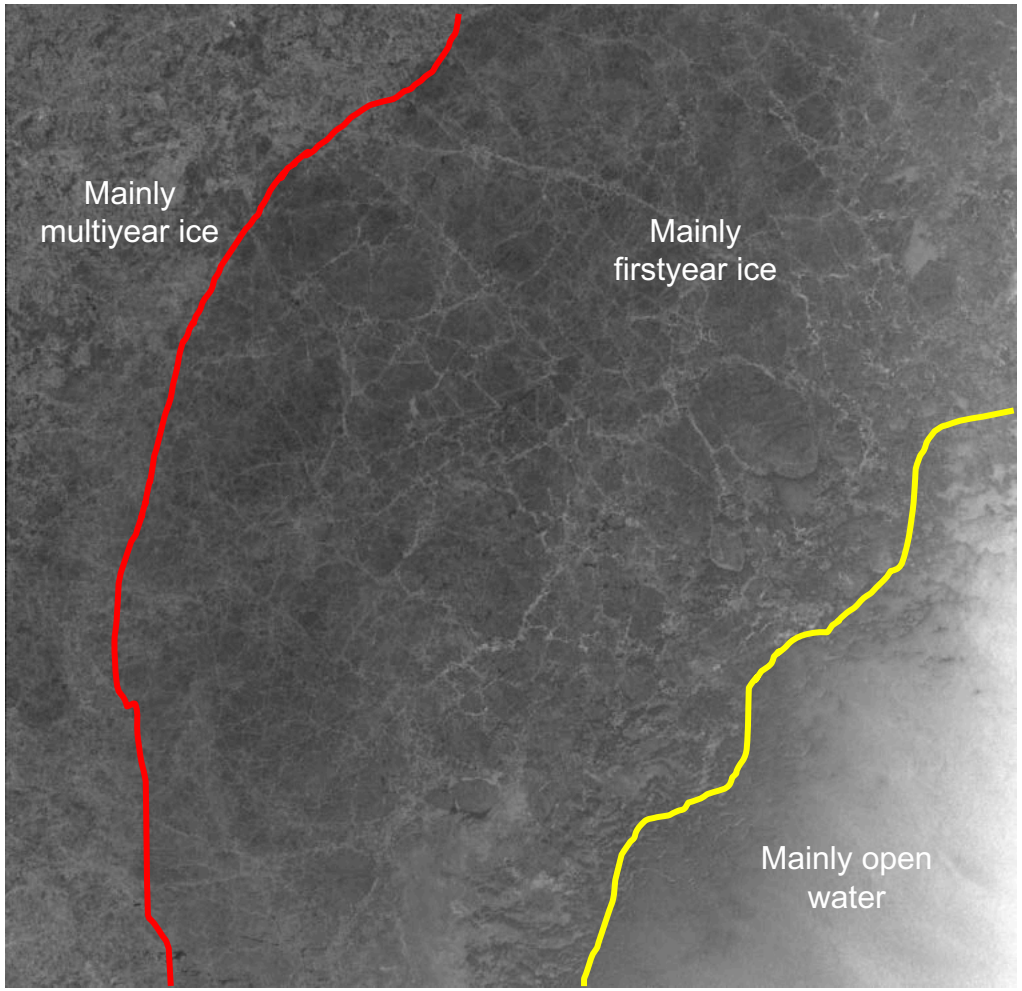

Sentinel-1 from Fram Strait, 12 June 2018, 07:27 (www.seaice.dk)

Backscatter versus incidence angle for ice types and open water

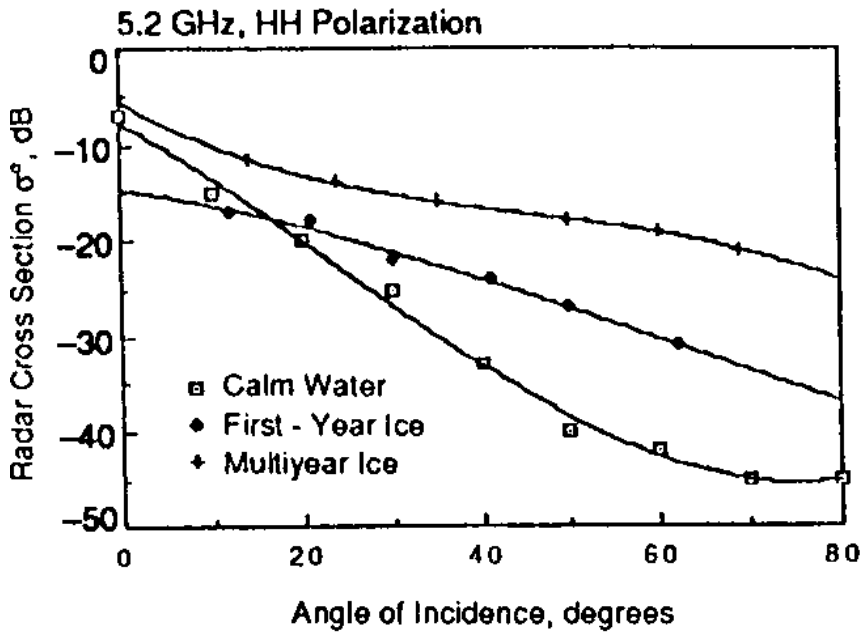

Winter

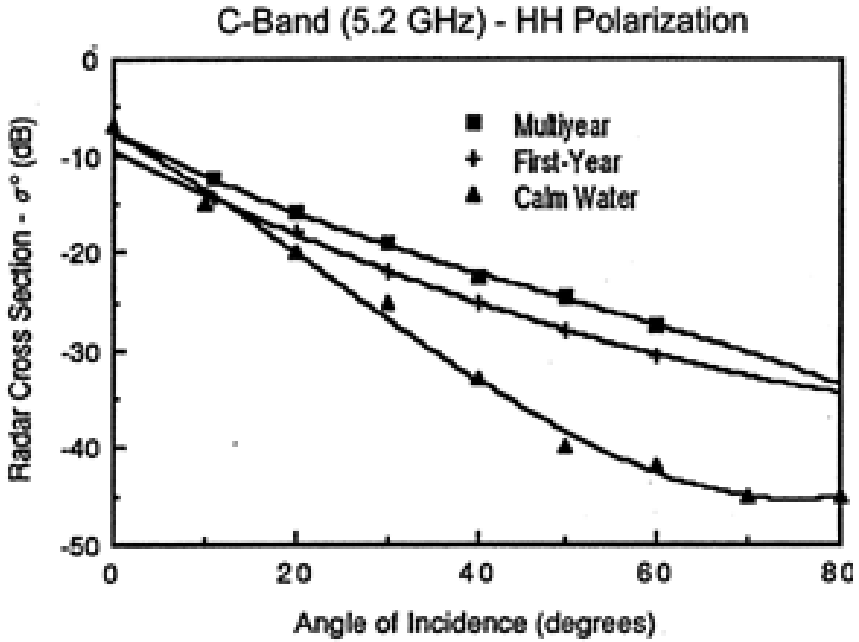

Summer

Backscatter statistics for the main ice types

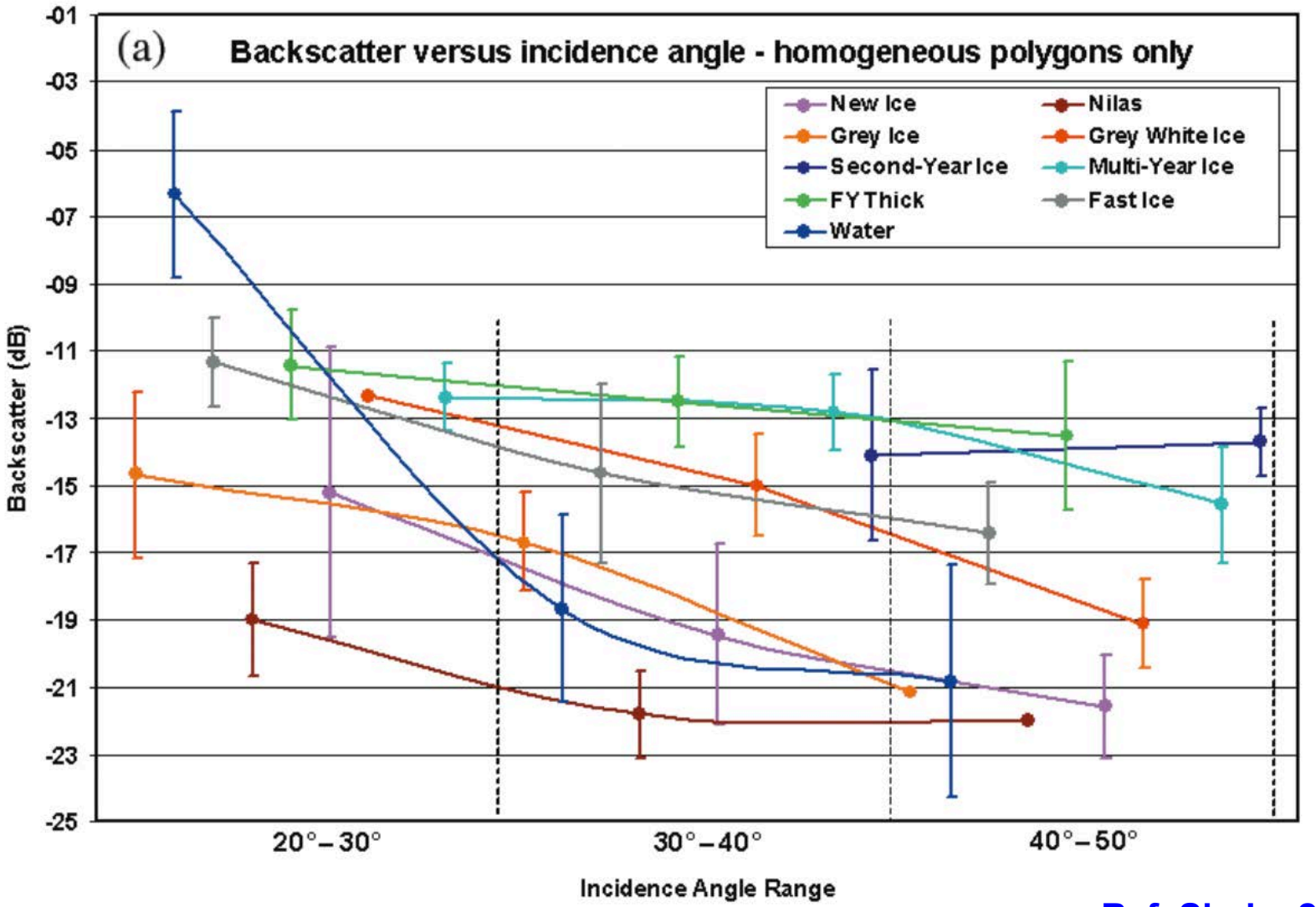

Ref. Shokr, 2006

Penetration depth of μ-waves

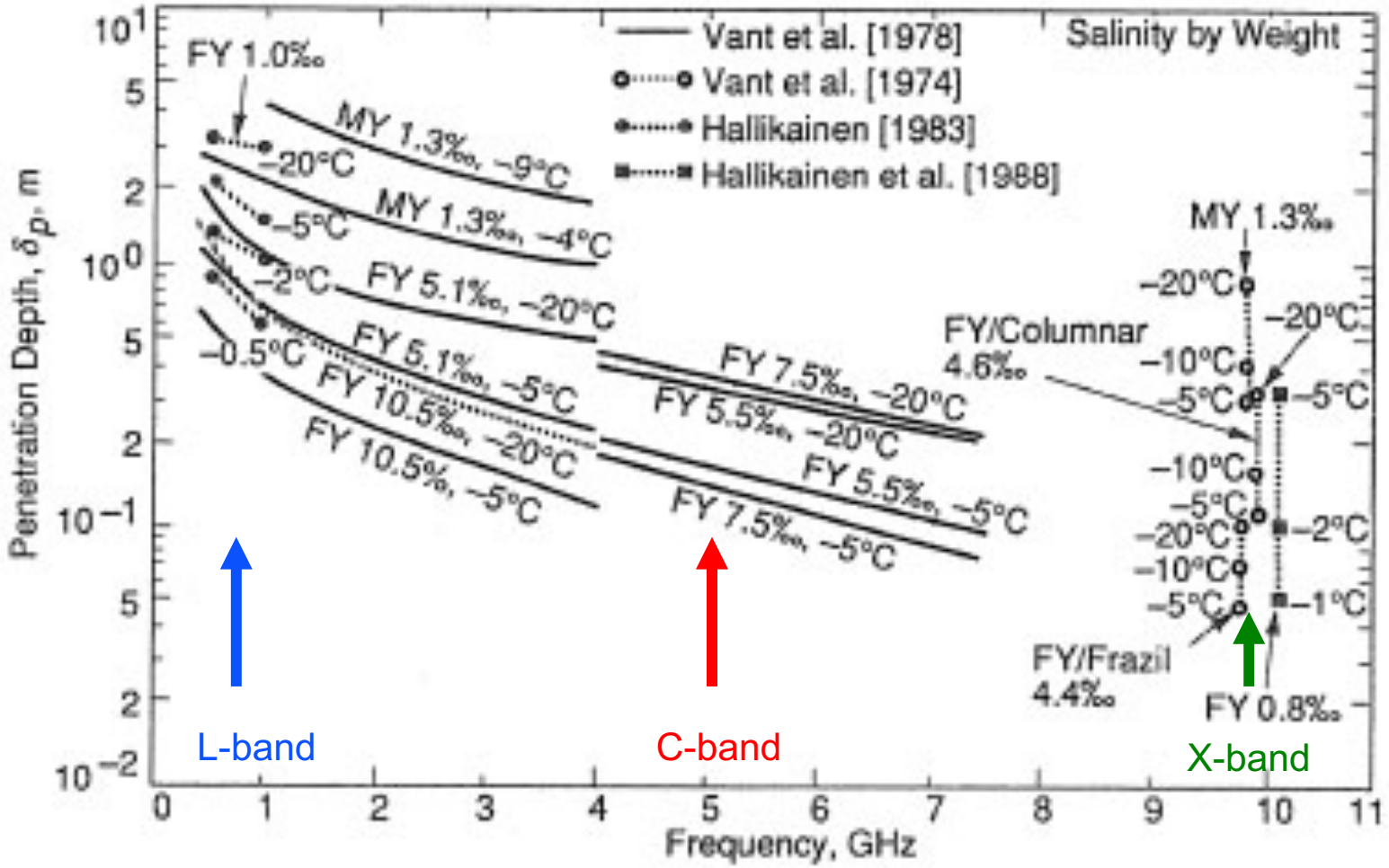

The penetration depth of μ-waves in sea ice increases with decreasing salinity and decreasing temperature

Profiles of temperature and salinity in ice

Thin FY ice

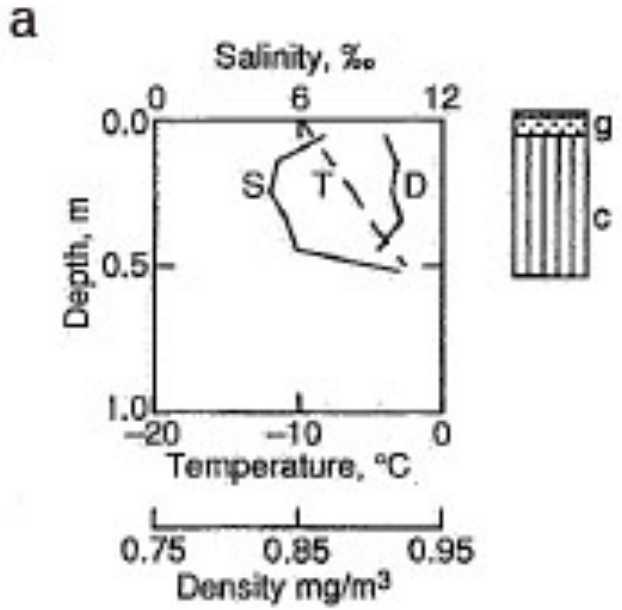

MY ice

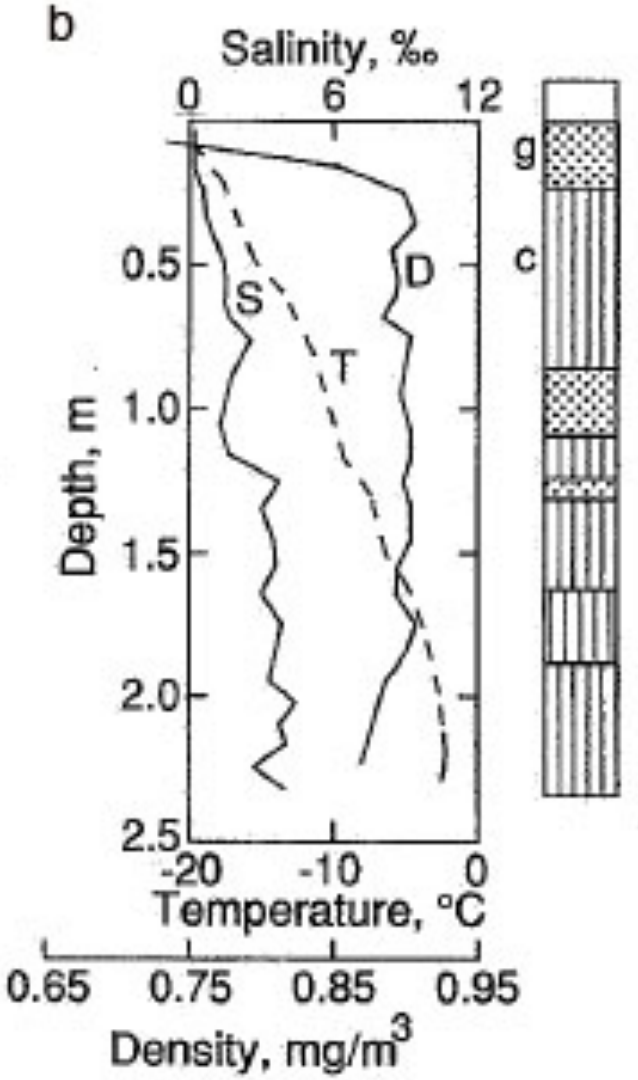

(Tucker, 1992)

Salinity of sea ice at different stage of development

Salinity for different stages of young ice

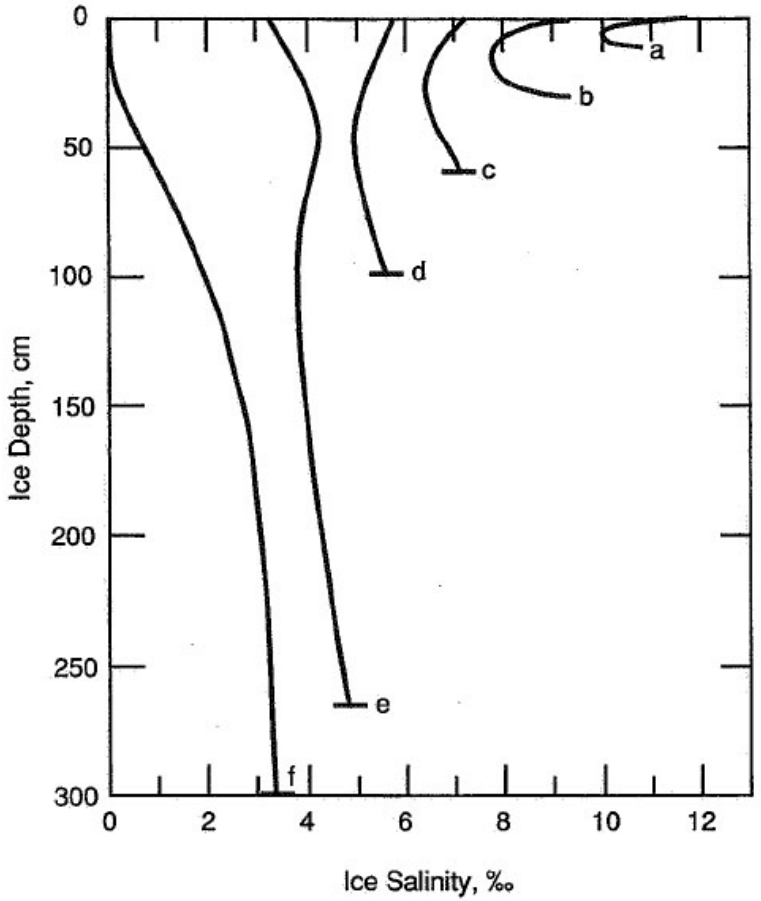

Salinity as function of ice thickness

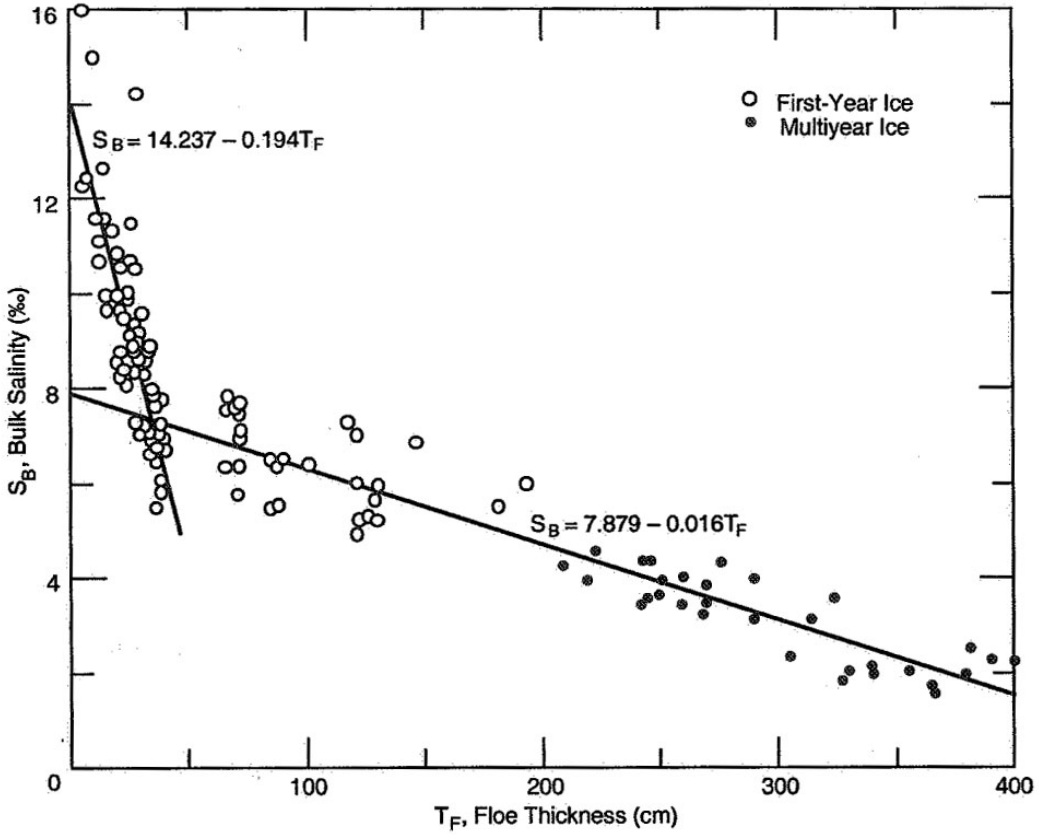

(Tucker, 1992)

SAR signal of sea ice in various frequencies and polarisations

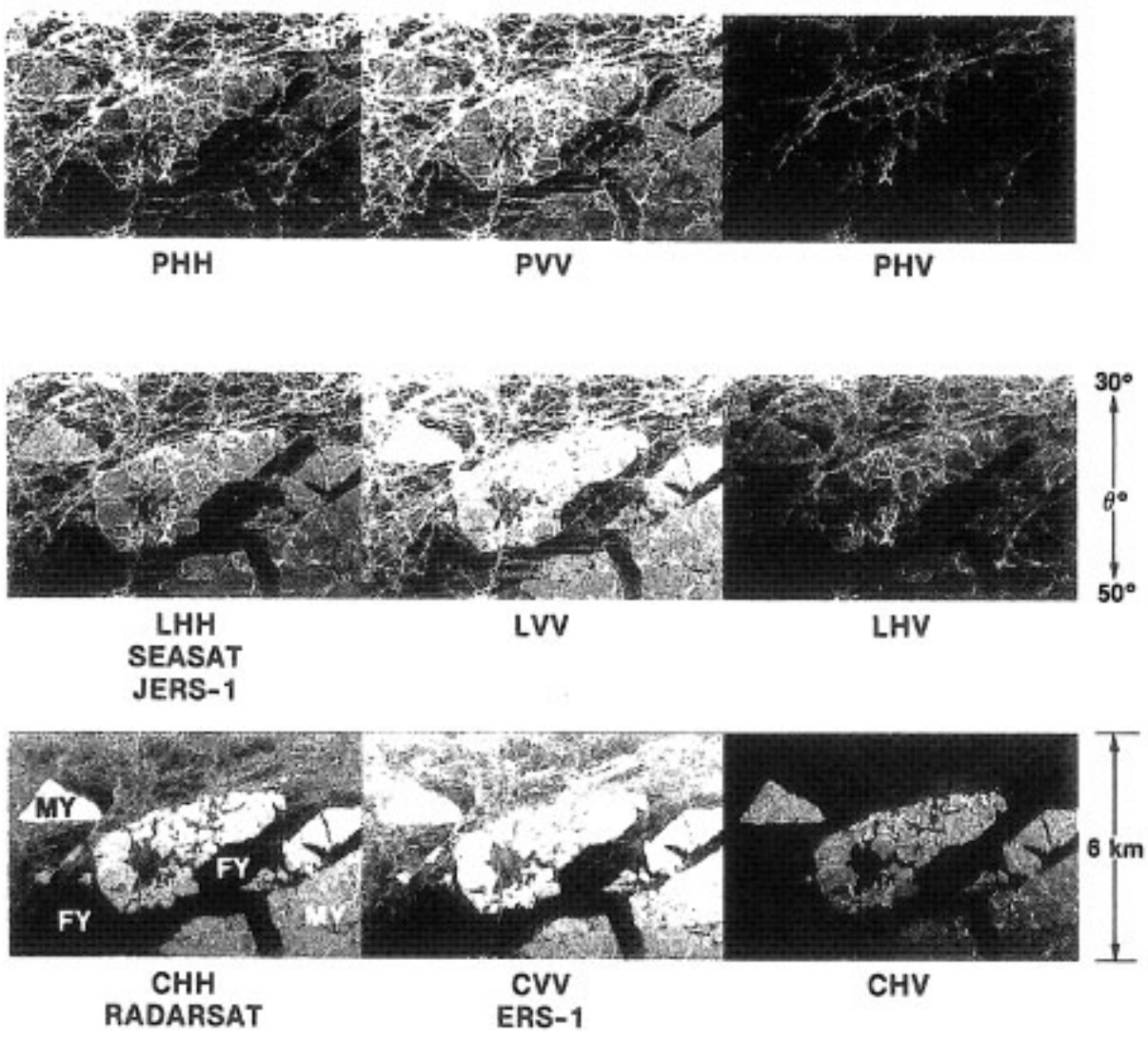

The same ice area imaged by different channels and polarisations.

NERSC

Comparison of VV (ERS) and HH (Radarsat) for the same sea ice area

C-band VV polarisation

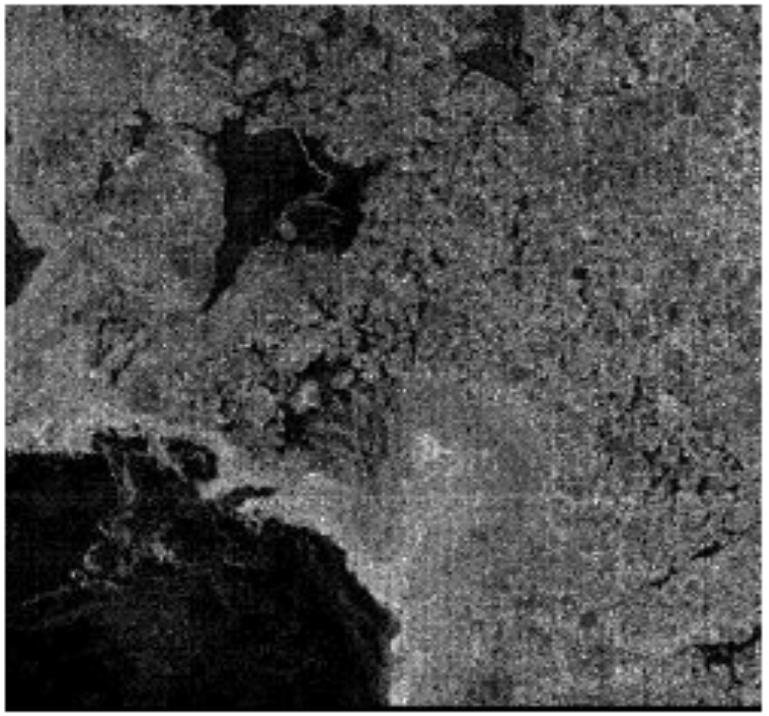

C-band HH polarisation

Comparison of SAR and optical images of sea ice

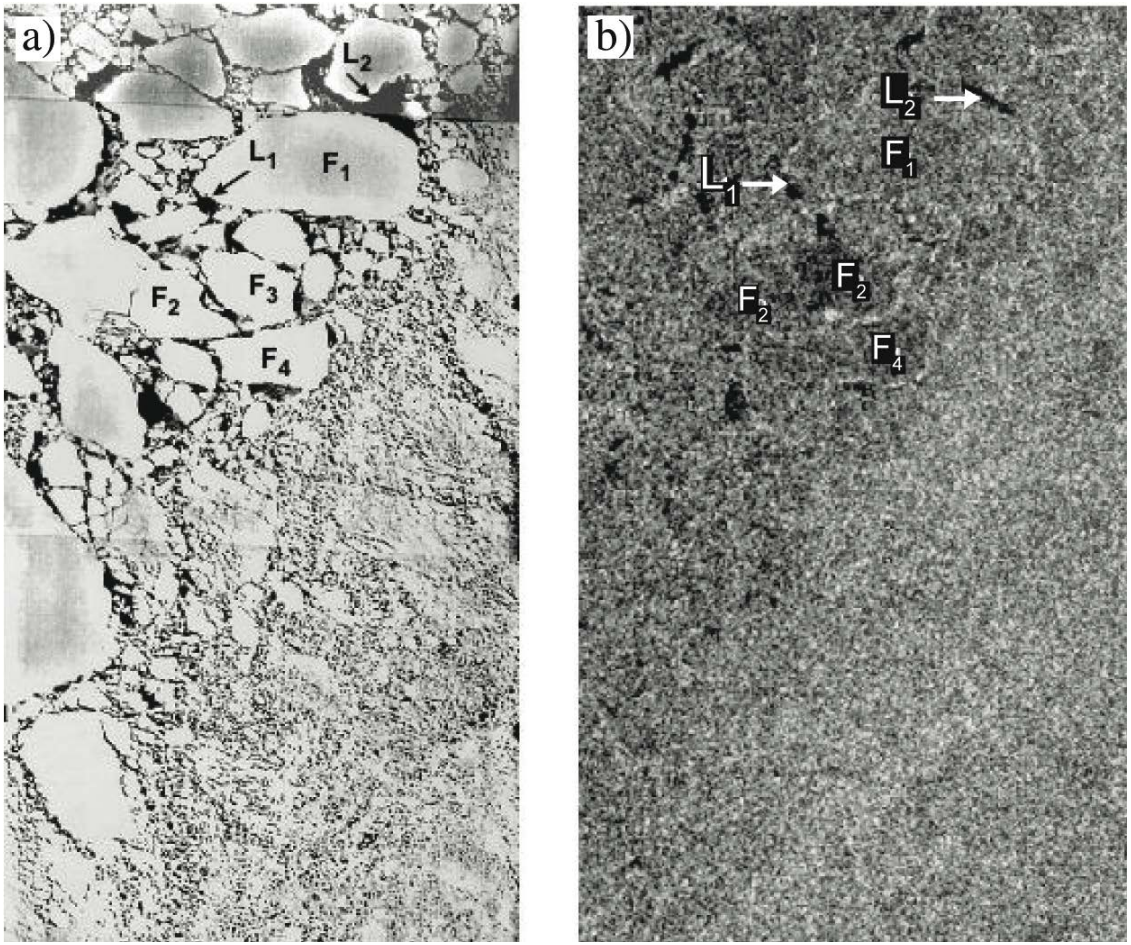

The same sea ice area of 4 km by 8 km and is mapped by vertical camera (a) and SAR image from ERS-1 (b)

Comparison of high-resolution SAR and optical images for ice deformation features

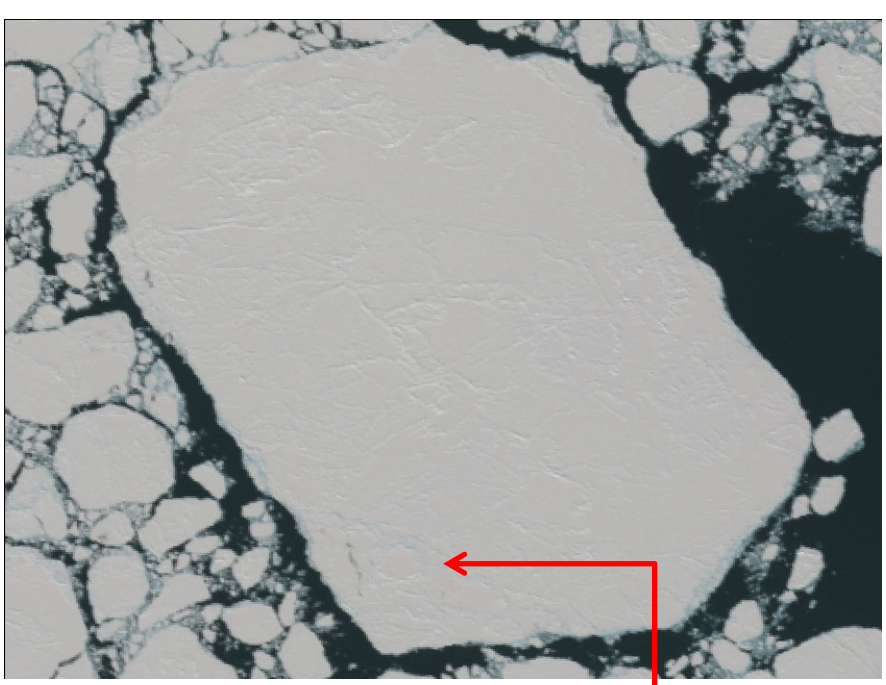

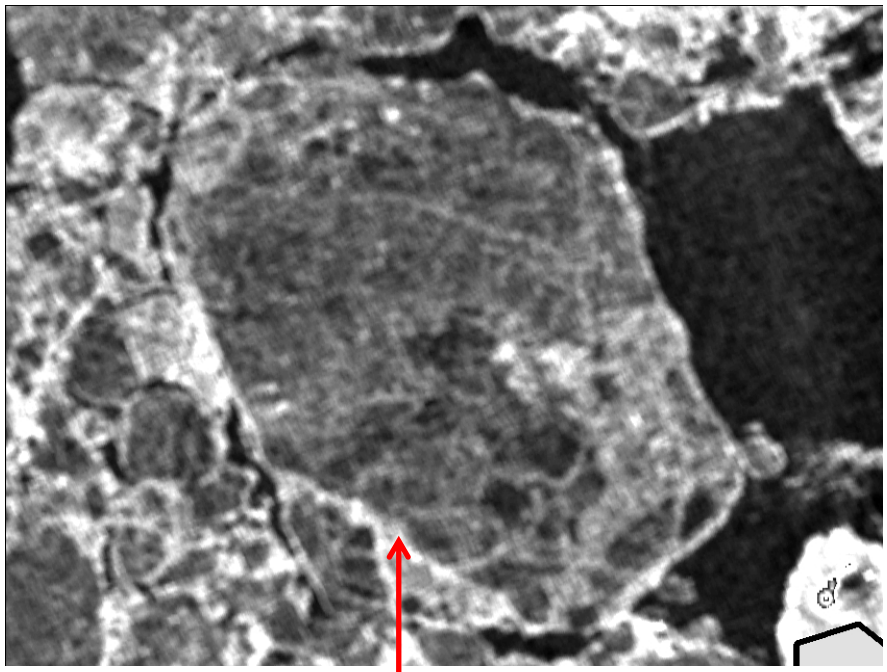

High-resolution optical image from SPOT

Ridge detection

Detection of ridges in C- and L-band images

Top row: SAR intensity images in C- and L-band from the Danish EMISAR. The images are

VV-polarisation

Bottom row: deformation maps from SAR image width (horizontal axis) is 1.5 km

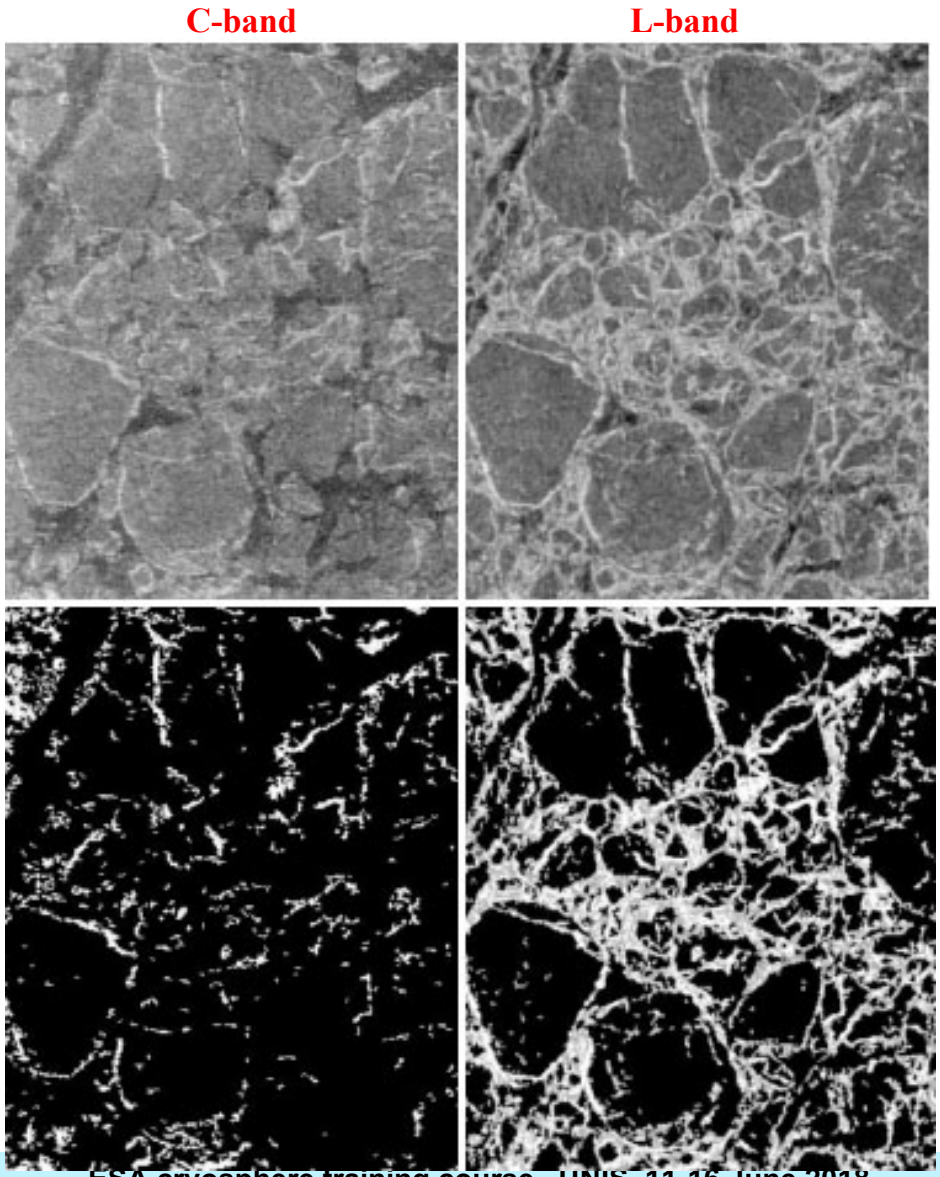

Courtesy: Dierking and Dall, 2007

Comparing C- and L-band SAR signature of ridges

Ref. F. A. Casey et al., 2016

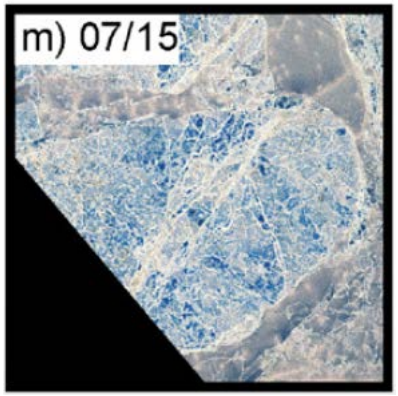

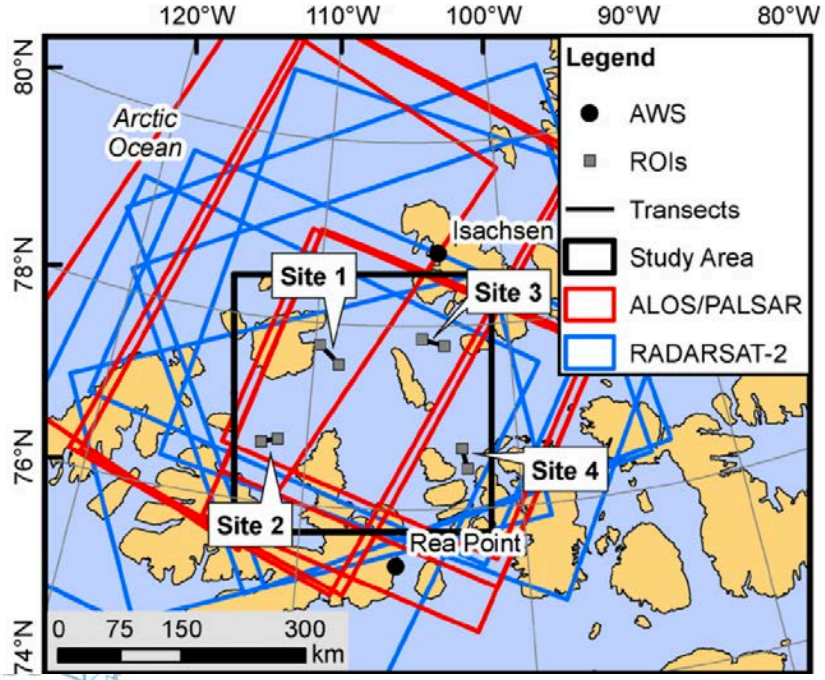

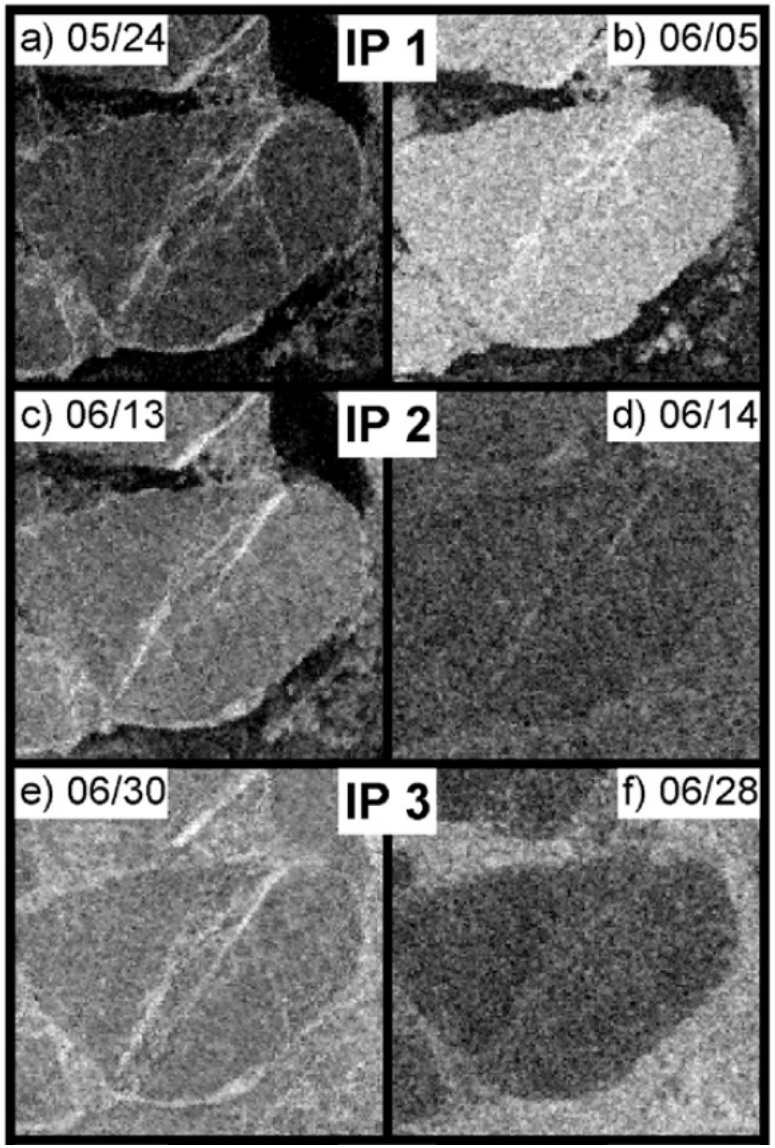

Ice edge variability and freezing in Hopen area

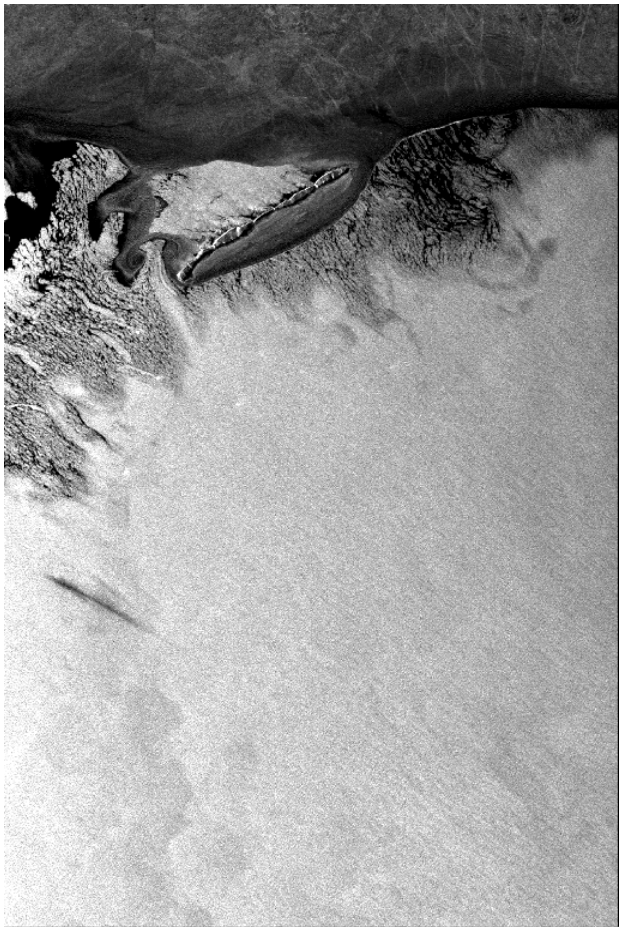

1 March 1992

4 March

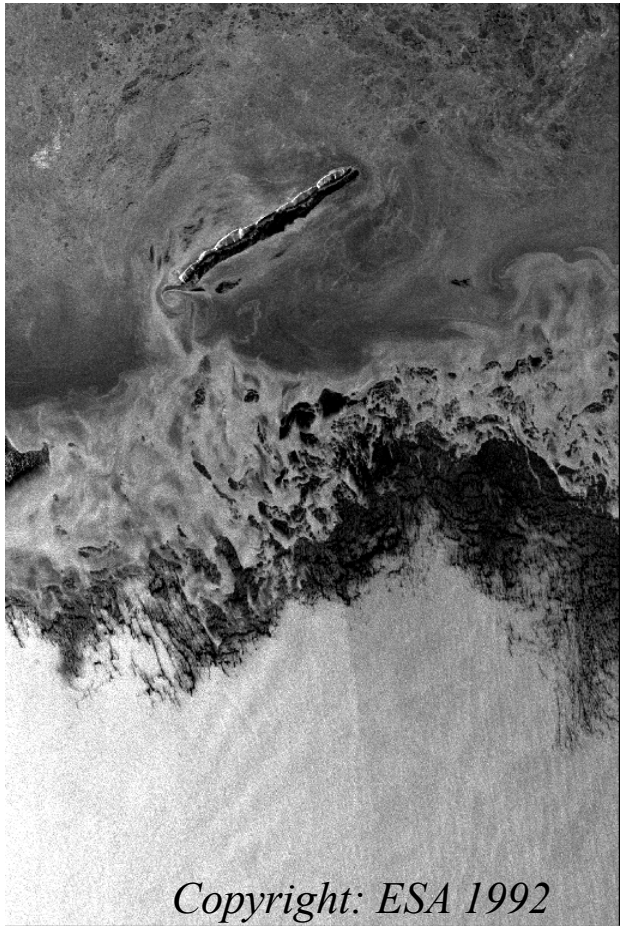

7 March

Ice freezing

Grease ice dampens the short surface waves - dark signature in SAR

Pancake ice gives a strong signature in SAR due to sharp edges.

SAR signature of grease ice and pancake ice

Photograph of the sea ice shown in the SAR image to the right

ERS-1 SAR in the Barents Sea March 1992, showing a mixture of grease ice, frazil and pancakes

SAR ice type classification based on backscatter (marginal ice zone in winter)

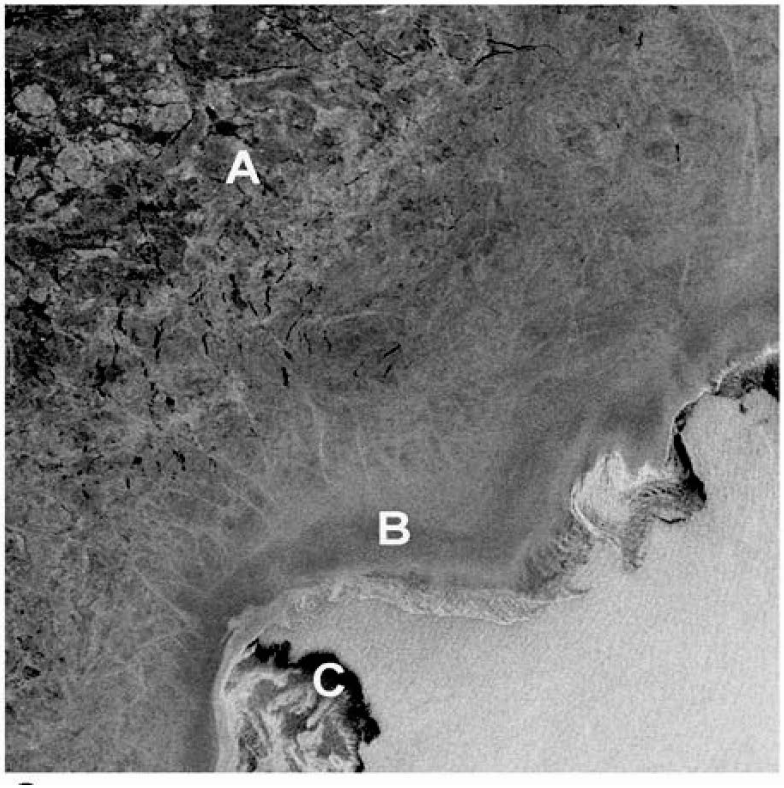

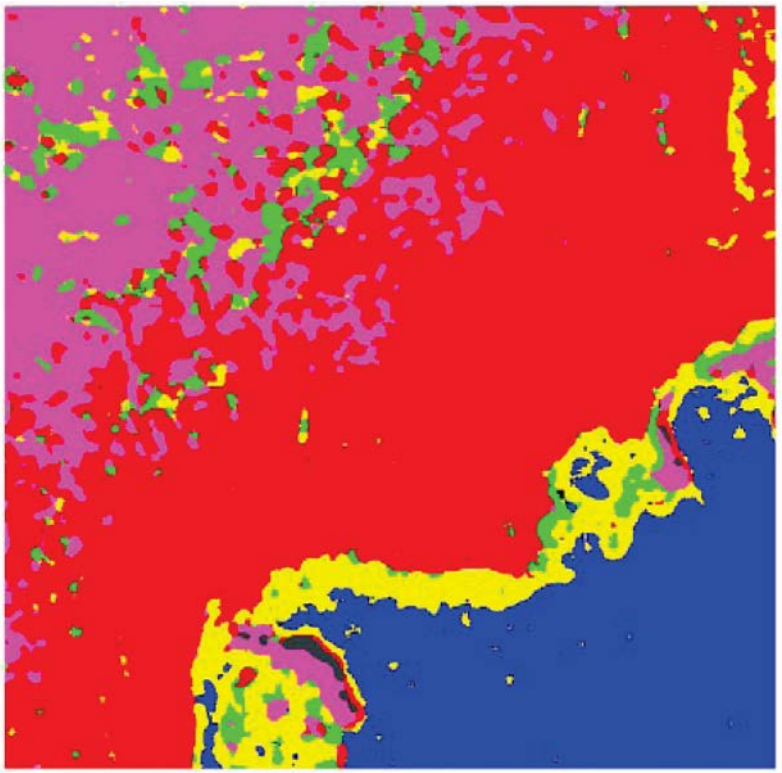

ERS-1 SAR in the Barents Sea March 1992

A: interior of the pack ice
B: marginal ice zone with small floes
C: freezing of new ice

Radar backscatter for different ice types and regions

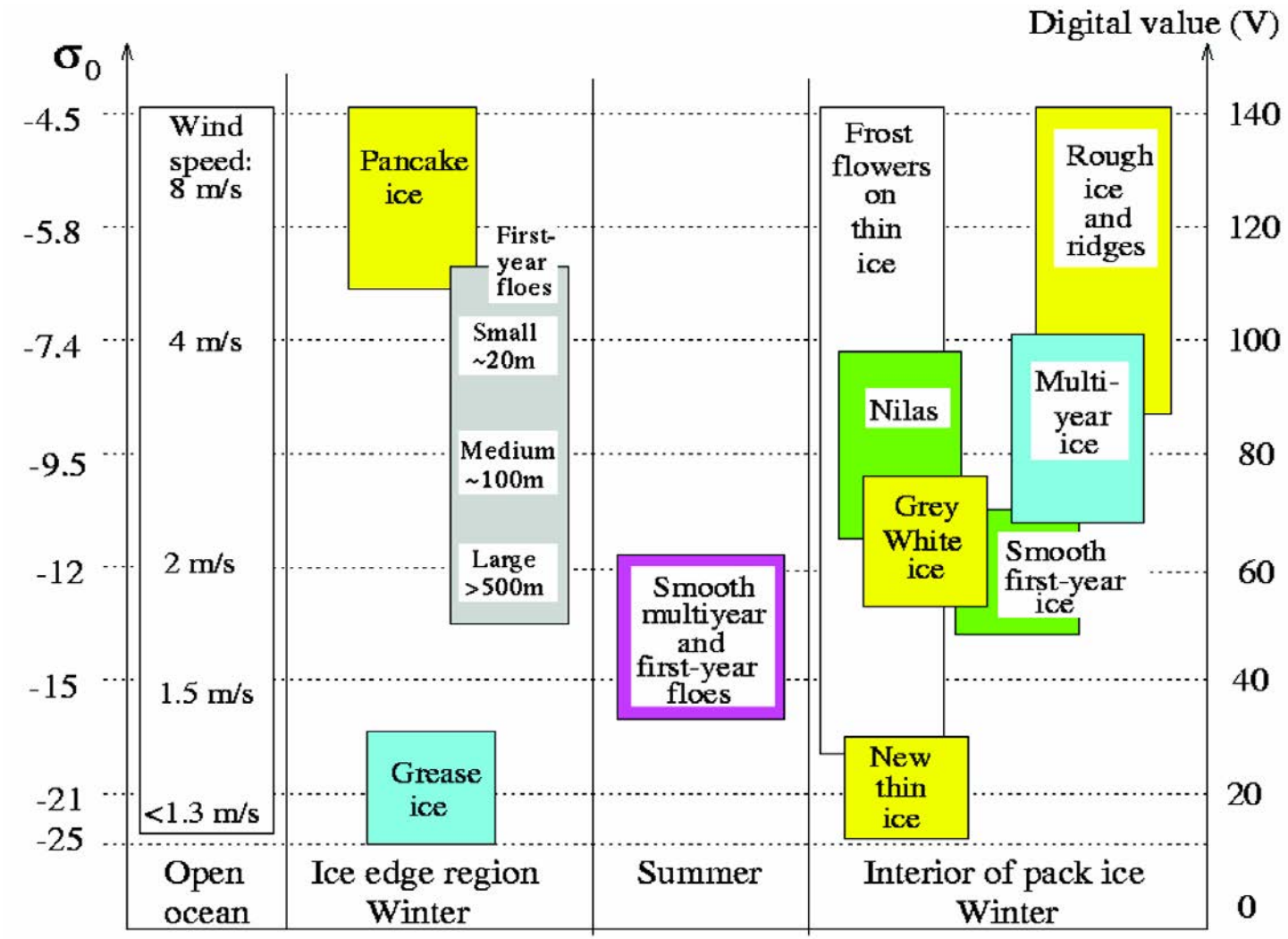

Sea ice evolution

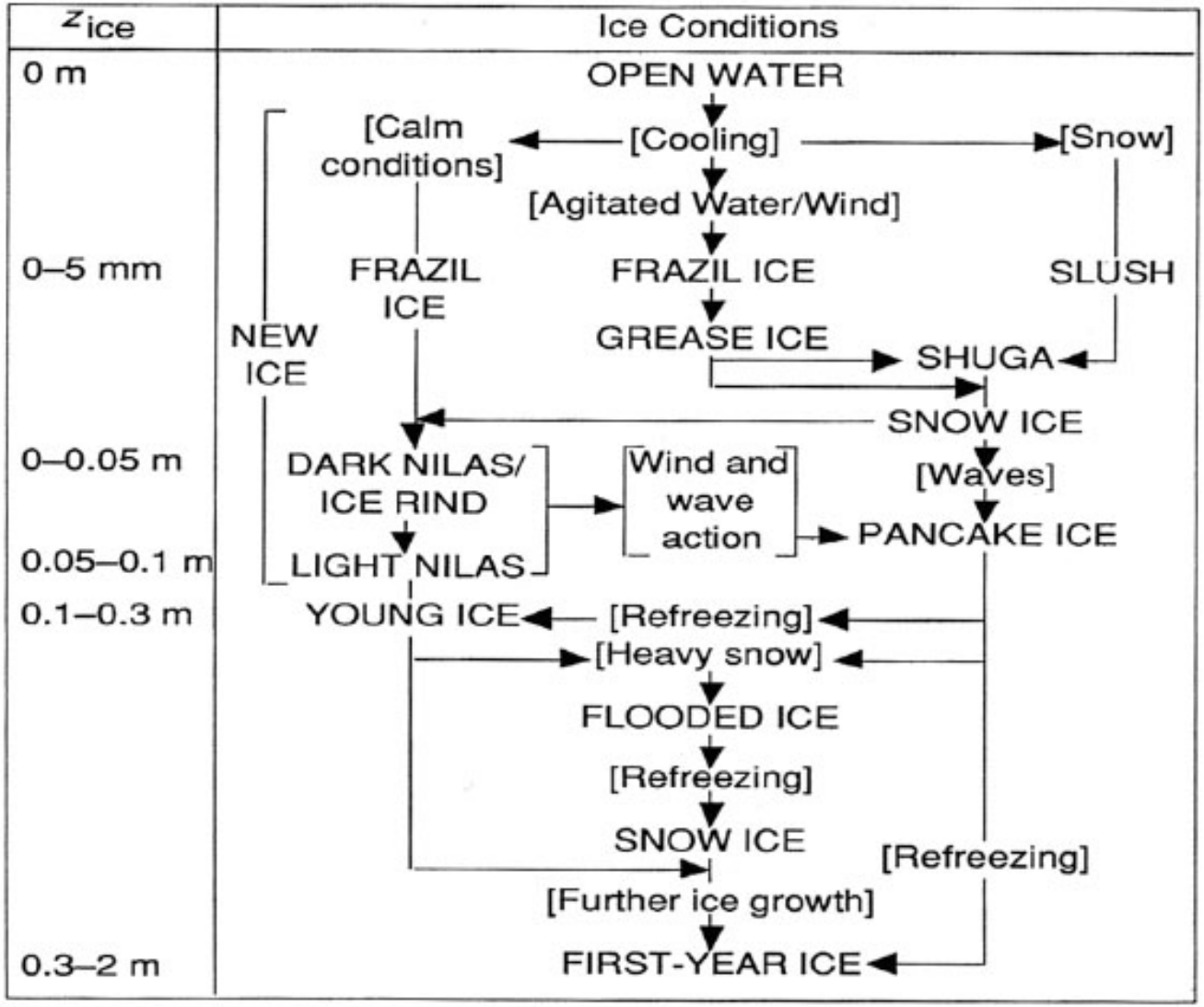

Melting of hummocks

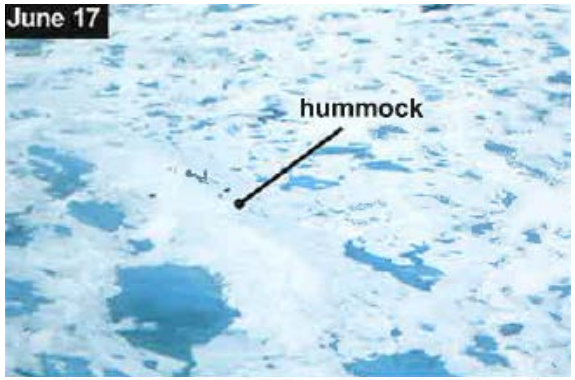

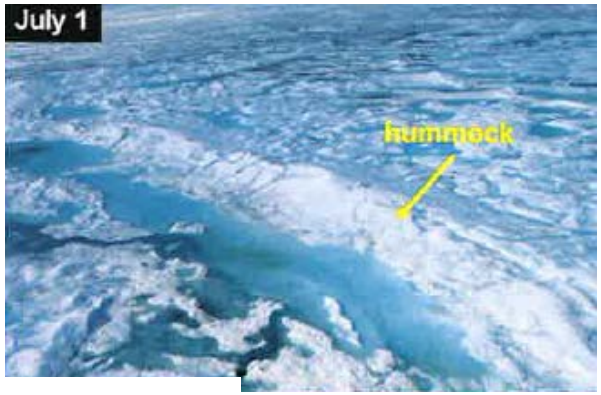

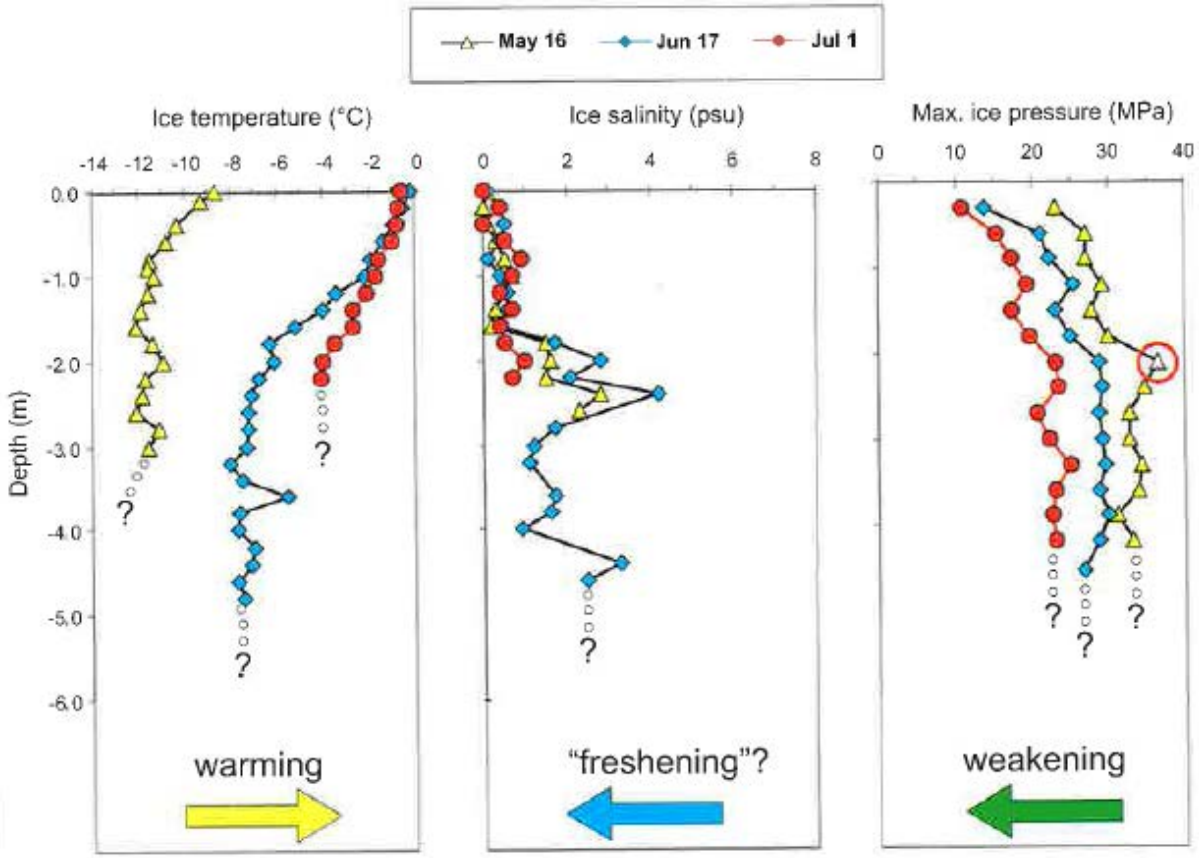

Ref. M. Johnson

SAR backscatter versus time evolution

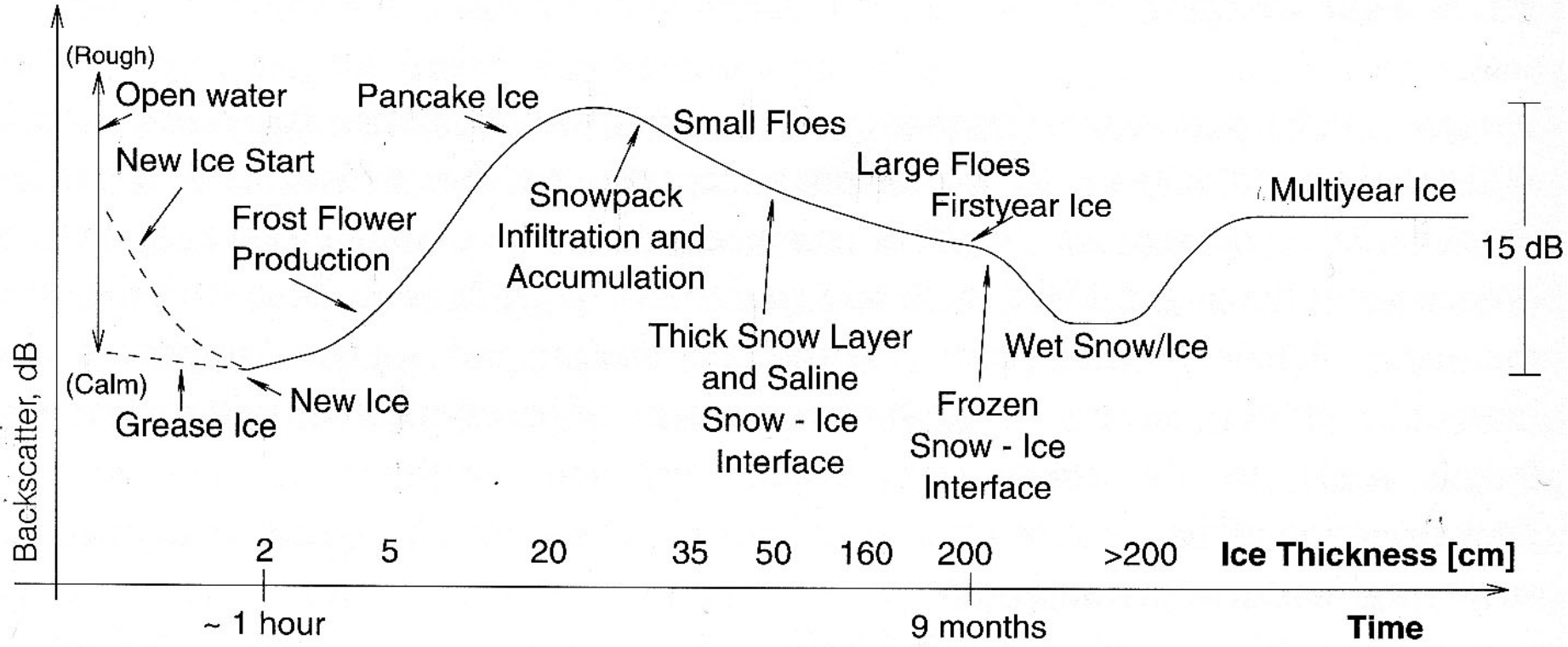

Classification of SAR images with Support Vector Machine algorithm

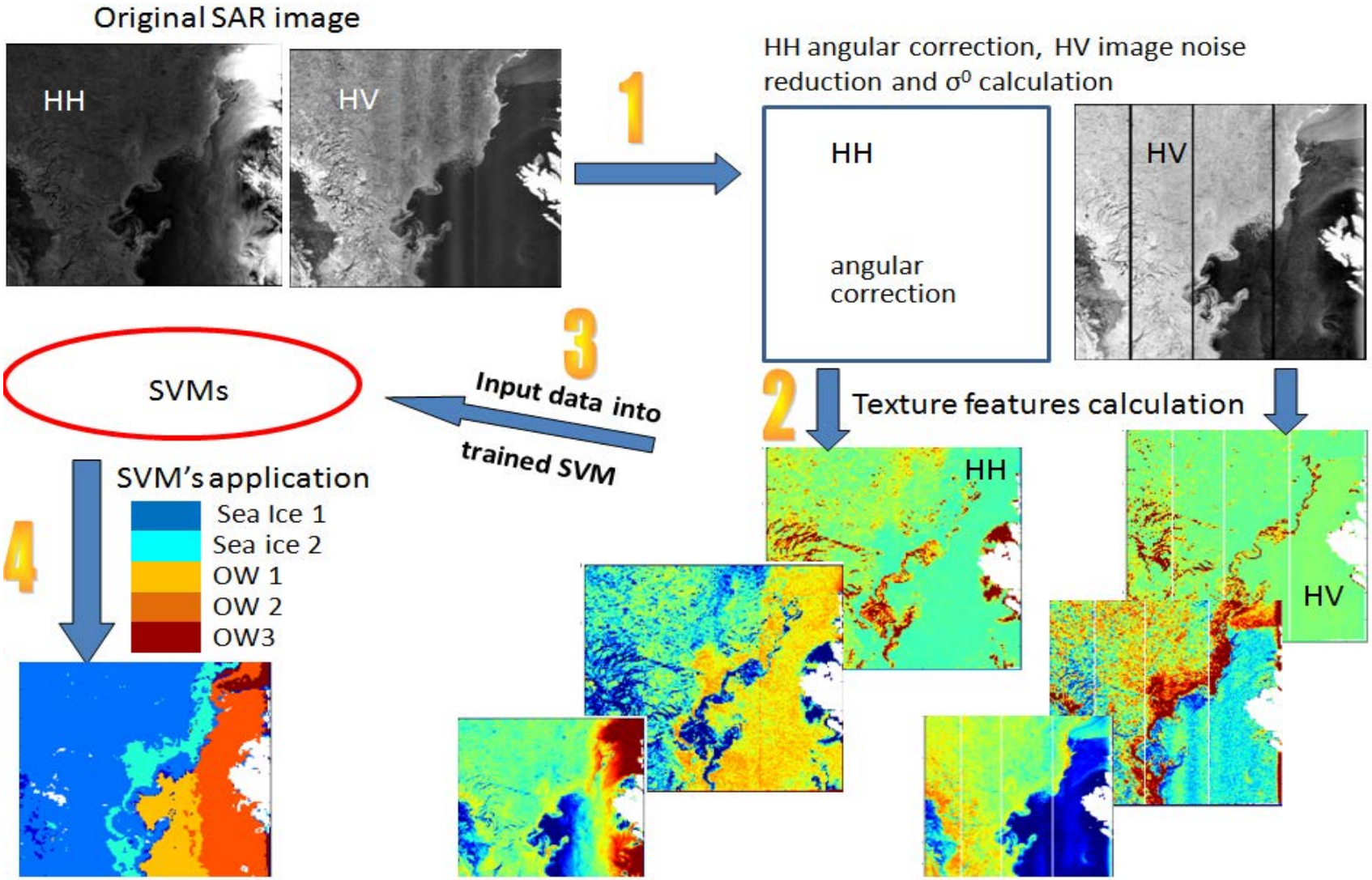

Zakhvatkina, N. et al. (2013).Classification of Sea Ice Types in ENVISAT Synthetic Aperture Radar Images, IEEE TRANSACTIONS ON GEOSCIENCE AND REMOTE SENSING, VOL. 51, NO. 5

Validation of sea ice classification results

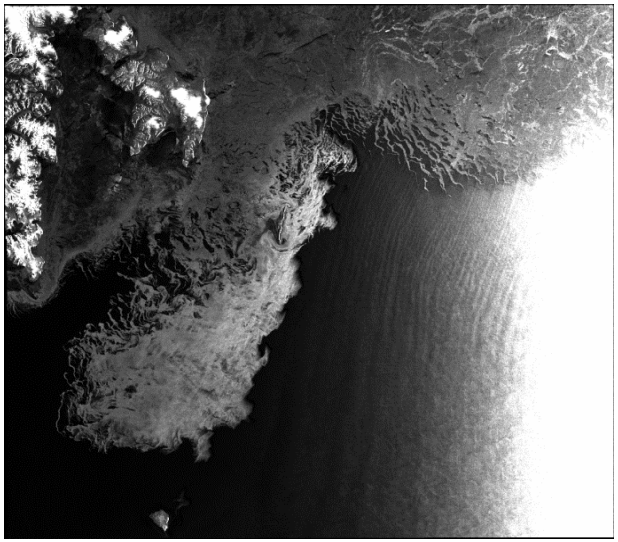

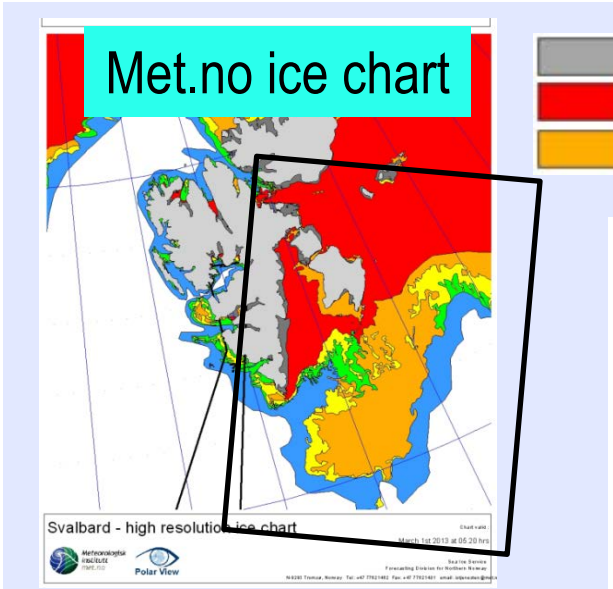

classification discrepancies:

ice met.no/OW SVM

OW met.no/ice SVM

No difference

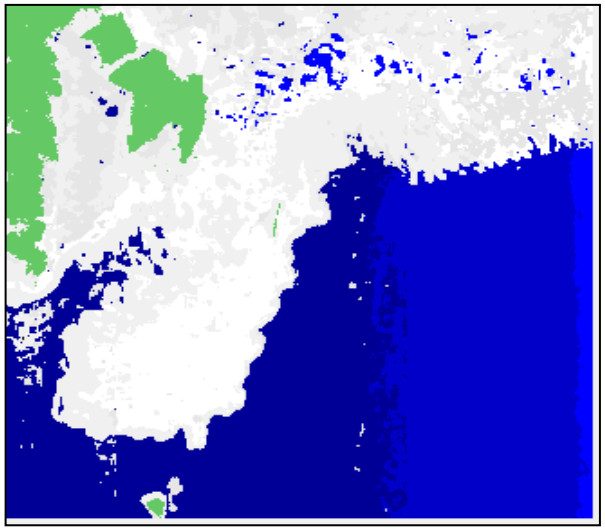

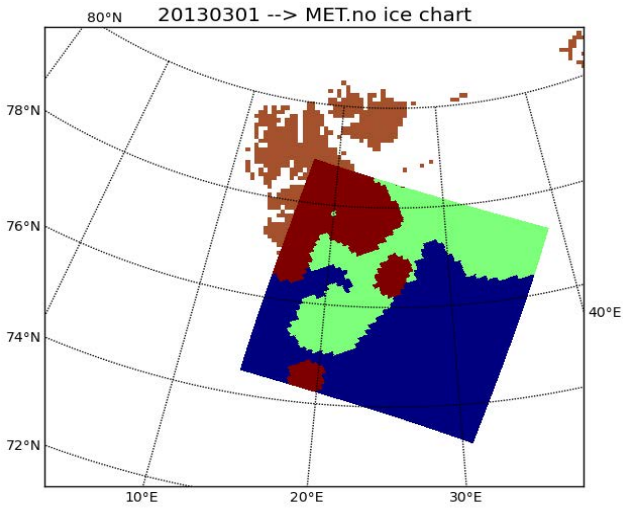

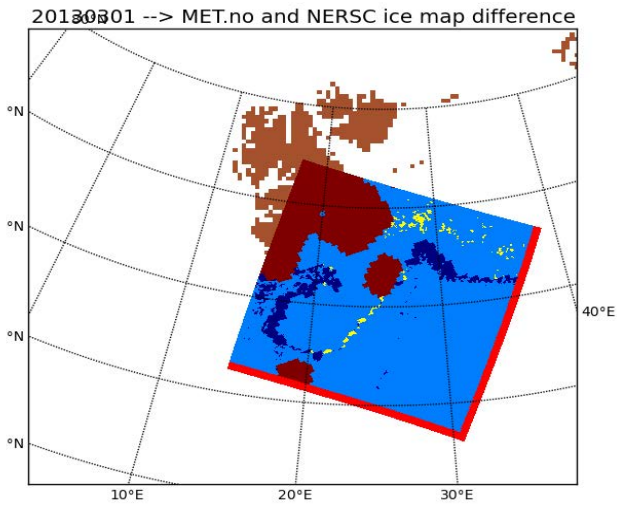

NERSC

Use of SAR in different resolution: Radarsat2 & Terra SAR-X

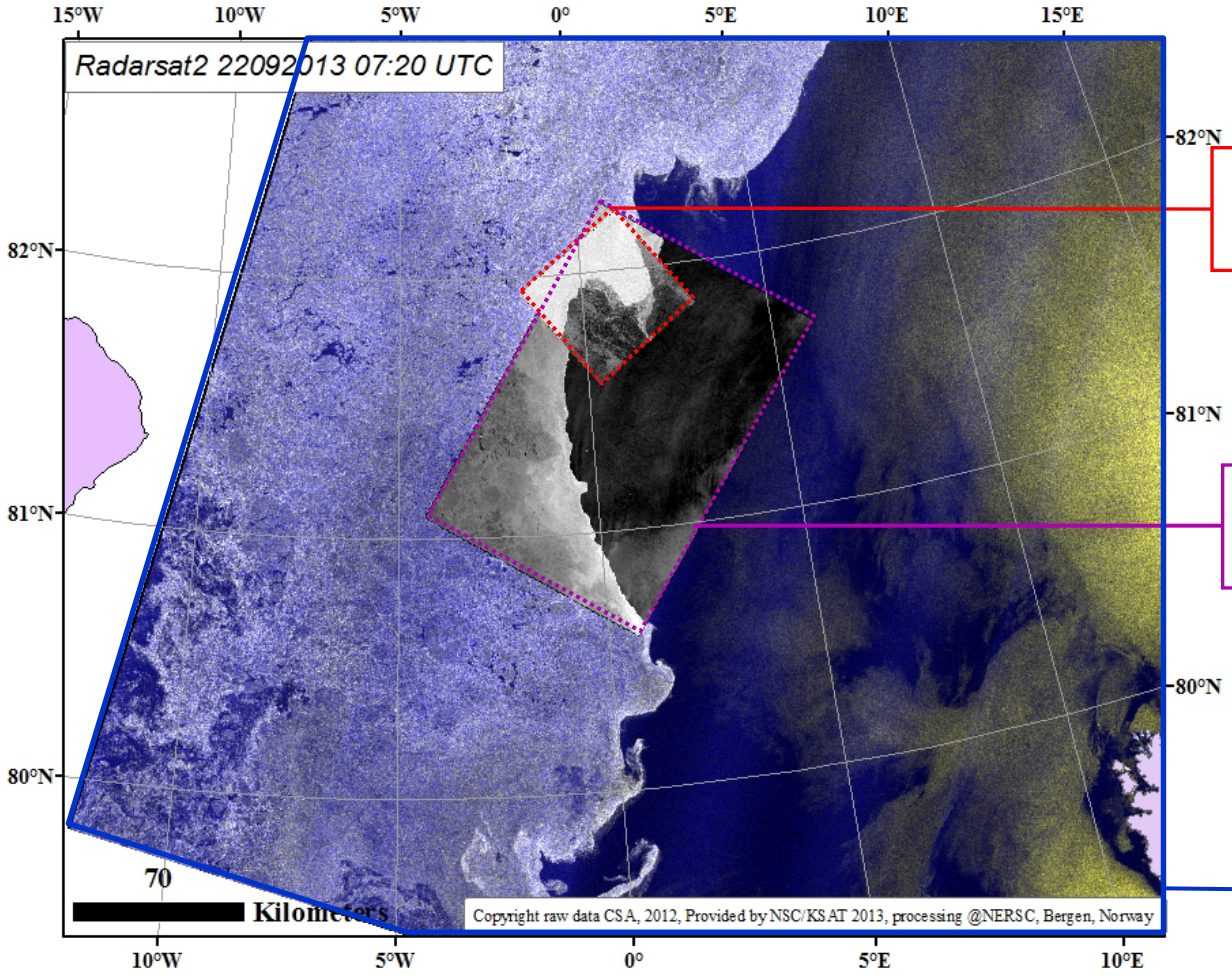

Radarsat2 Fine dual Pol
22092013 15:41

Terra SAR-X Scan SAR
22092013 08:09

Radarsat2 Scan SAR Wide
22092013 07:20

Terra SAR-X Scan SAR, Fram Strait 20.09 - 2013 08:09

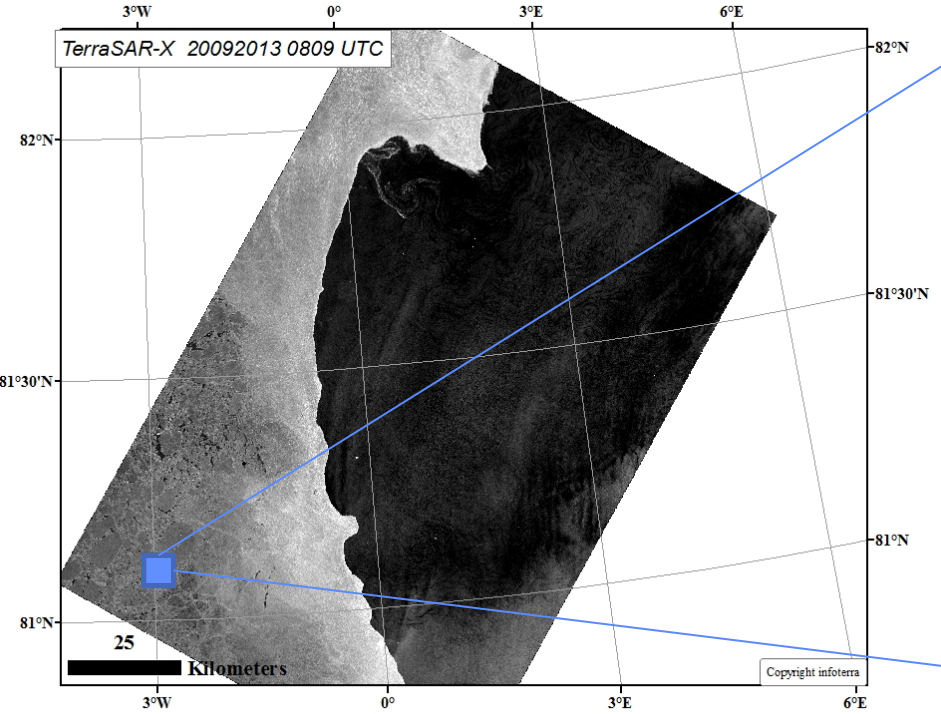

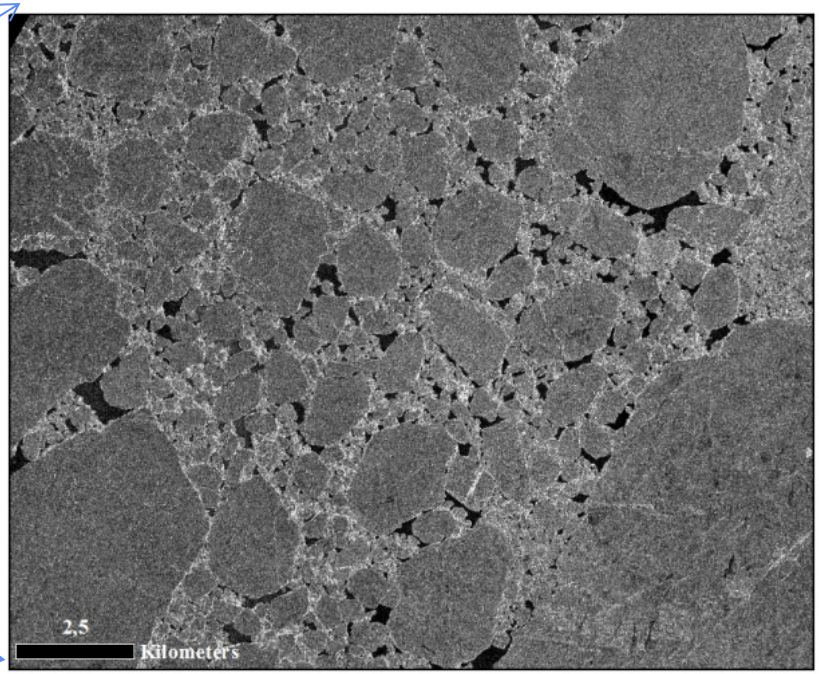

Example of high resolution image in the Fram Strait

(Radarsat2 Fine dul Pol), 22.09-2013 15:41

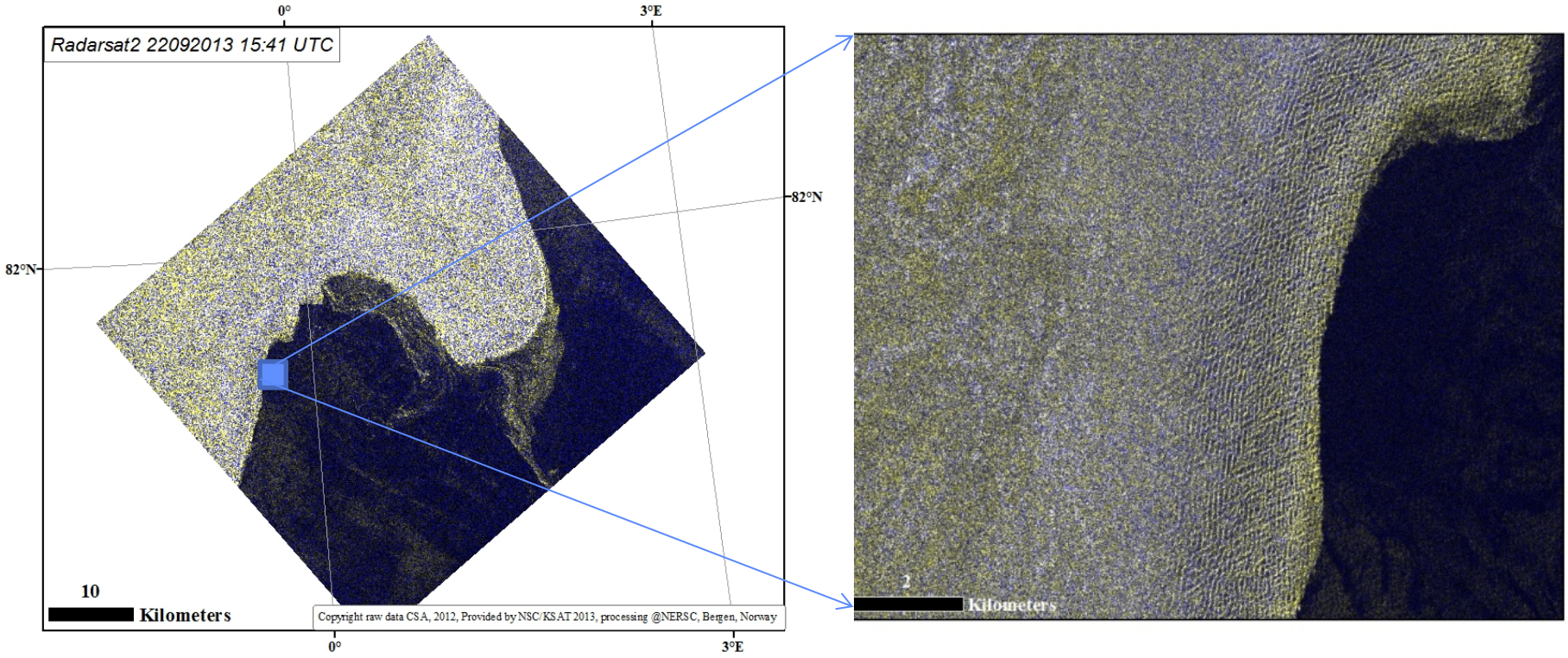

Ice drift in the Fram Strait from SAR images

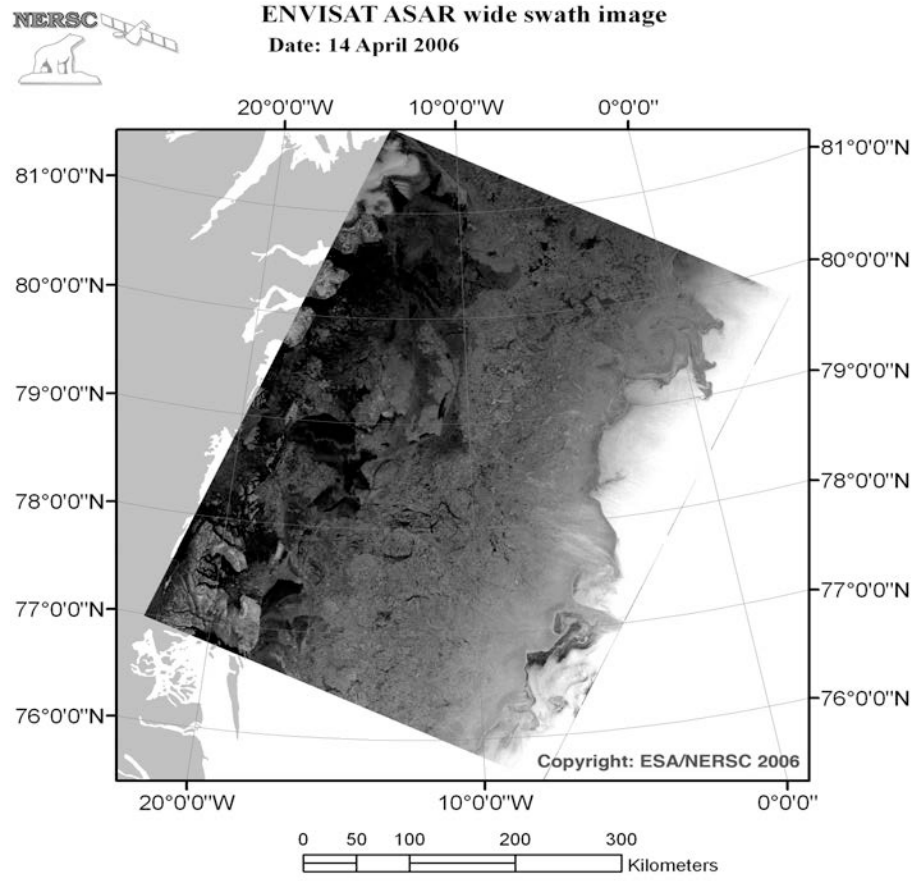

Data source: ENVISAT ASAR wide swath
Resolution: 100 meters
Orbits: 21549,
Projection:Lambert_Azimuthal_Equal_Area

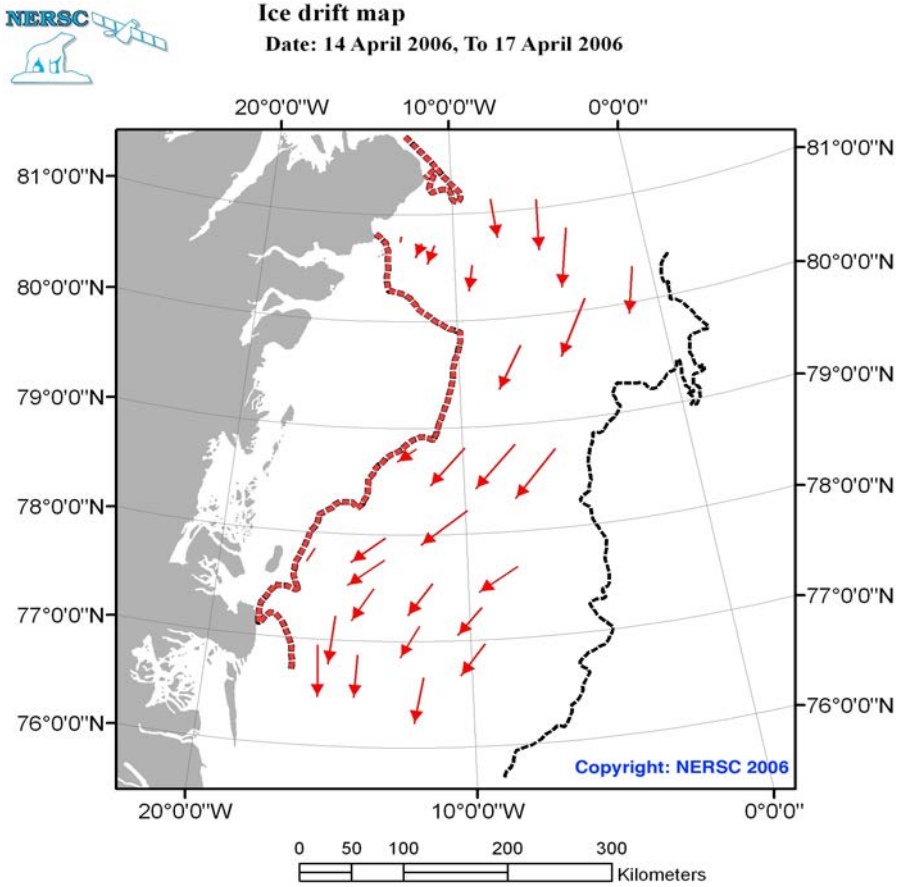

Legend

Ice edge, date 14 April 2006

Fast_ice edge

Ice drift scale

0.2 m/s

Data source: ENVISAT ASAR wide swath
Resolution: 100 meters
Orbits: 21549, 21592
Projection:Lambert_Azimuthal_Equal_Area

Automated algorithm for sea Ice drift from Sentinel-1 images

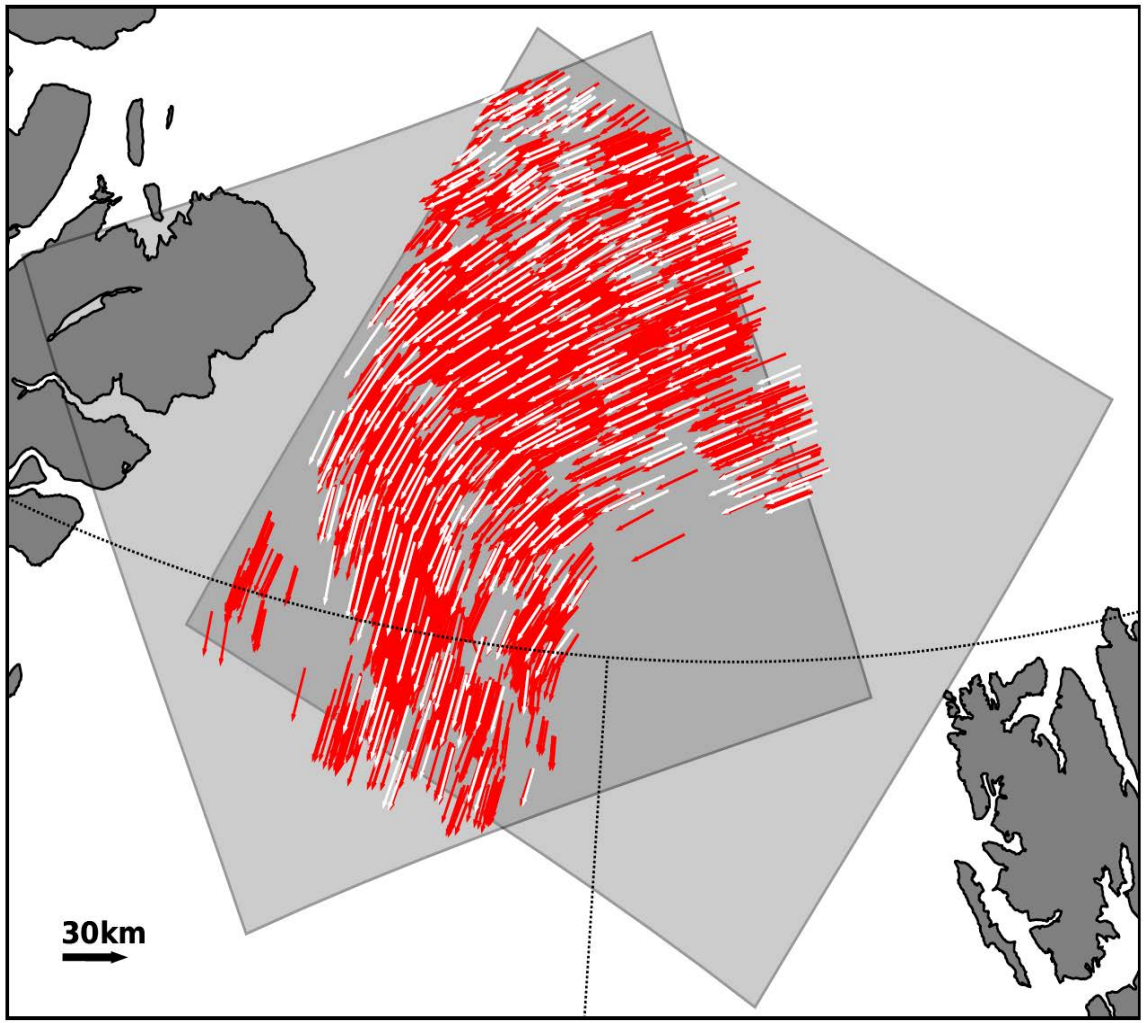

Analysed 1500 SAR images over 18 months, both HH and HV

Max interval between image pairs 72 hours

Feature trackimg algorithm (Muckenhuber et al., 2016)

Ref. Muckenhuber et al., 2016

CosmoSkymed image of sea ice with of near 100 % concentration (5 m resolution)

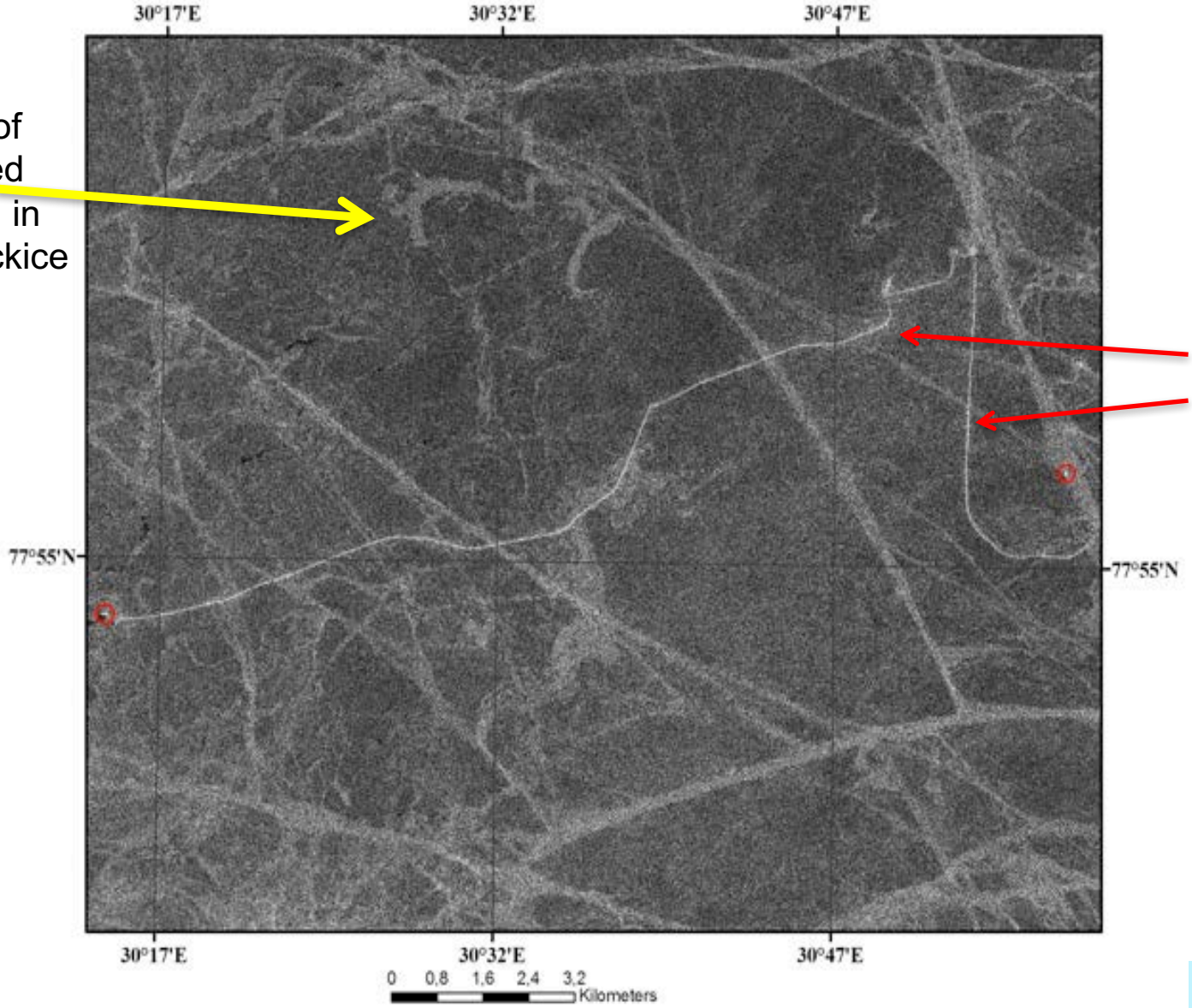

Tracks of grounded icebergs in drifting packice

15 May 2009

Barents Sea

Ship tracks in ice

NERSC

Nansen Environmental and Remote Sensing Center

Thormøhlensgate 47, N-5006 Bergen, Norway
http:www.nersc.no

Ice analysis and description

Date: 16 Jan 2006

Data source: ENVISAT ASAR wide swath
Resolution: 100 meters
Orbits: 20243, 20286
Projection:Transverse_Mercator

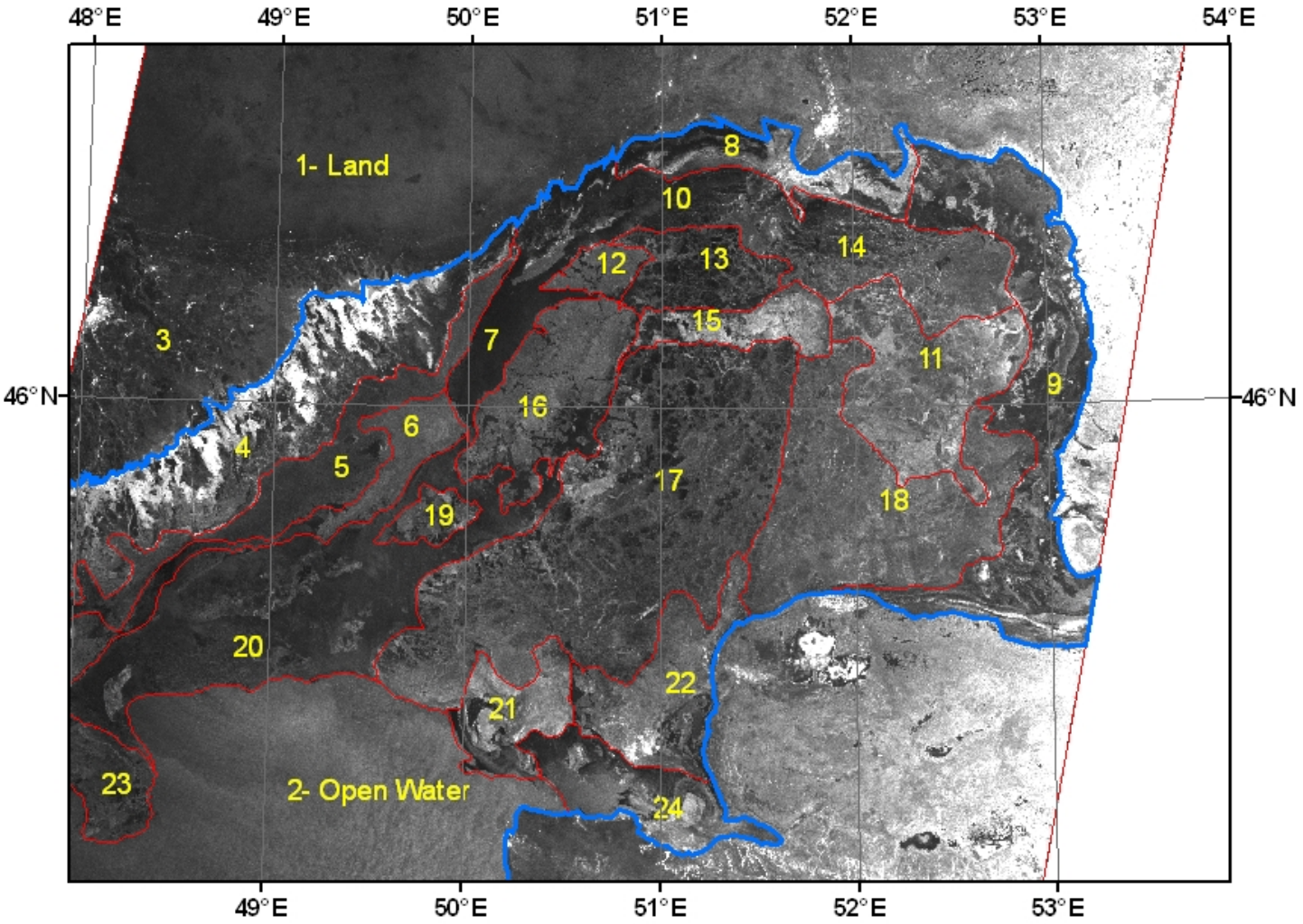

Ice navigation in thin ice along the Yamal peninsula using SAR data

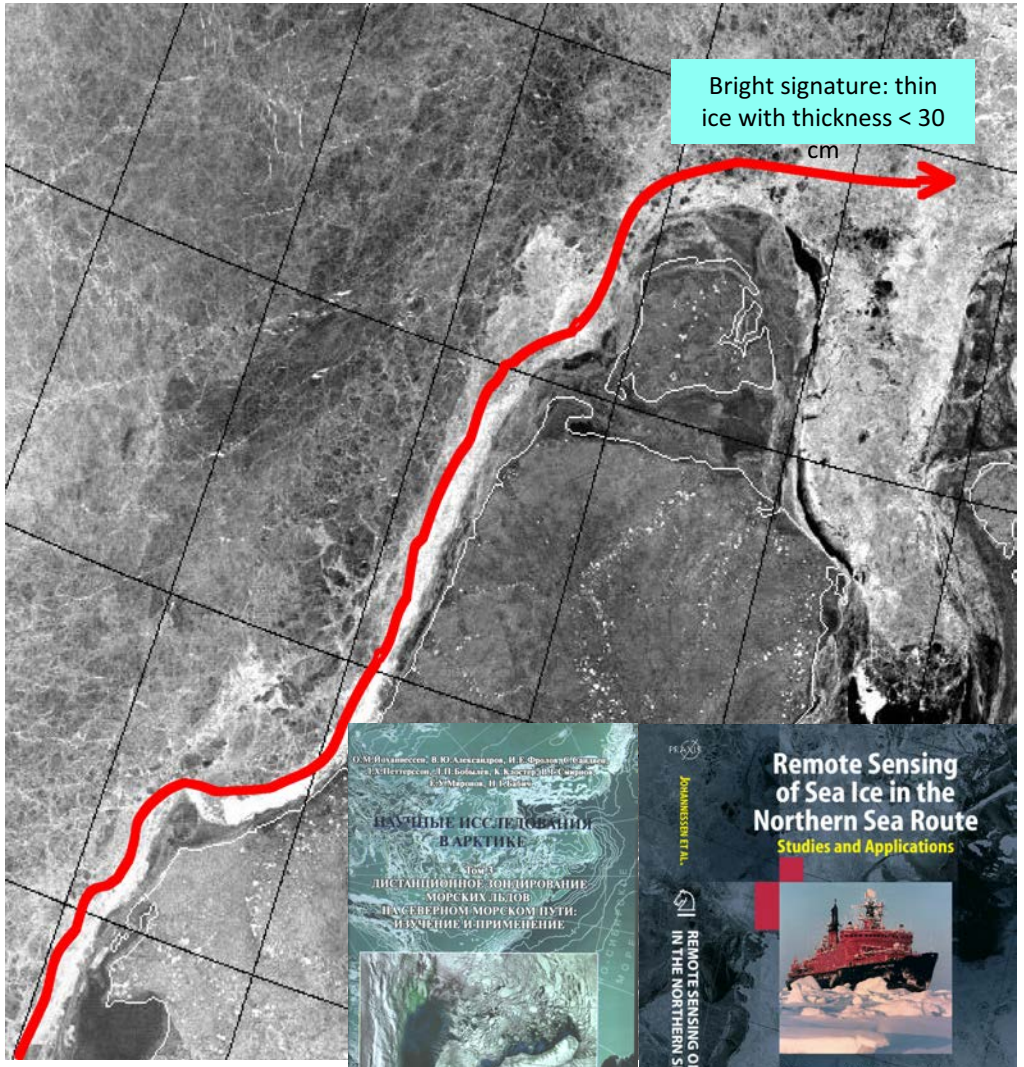

Russian-Norwegian cooperation since 1992:

Nuclear icebreaker Rossia sailed along the Yamal coast in June 2003 (red line).

SAR imagery from ENVISAT were used to analyze the sea ice and find the optimal sailing route.

Use of SAR data during the ARCDEV expedition in the Kara Sea in April 1998

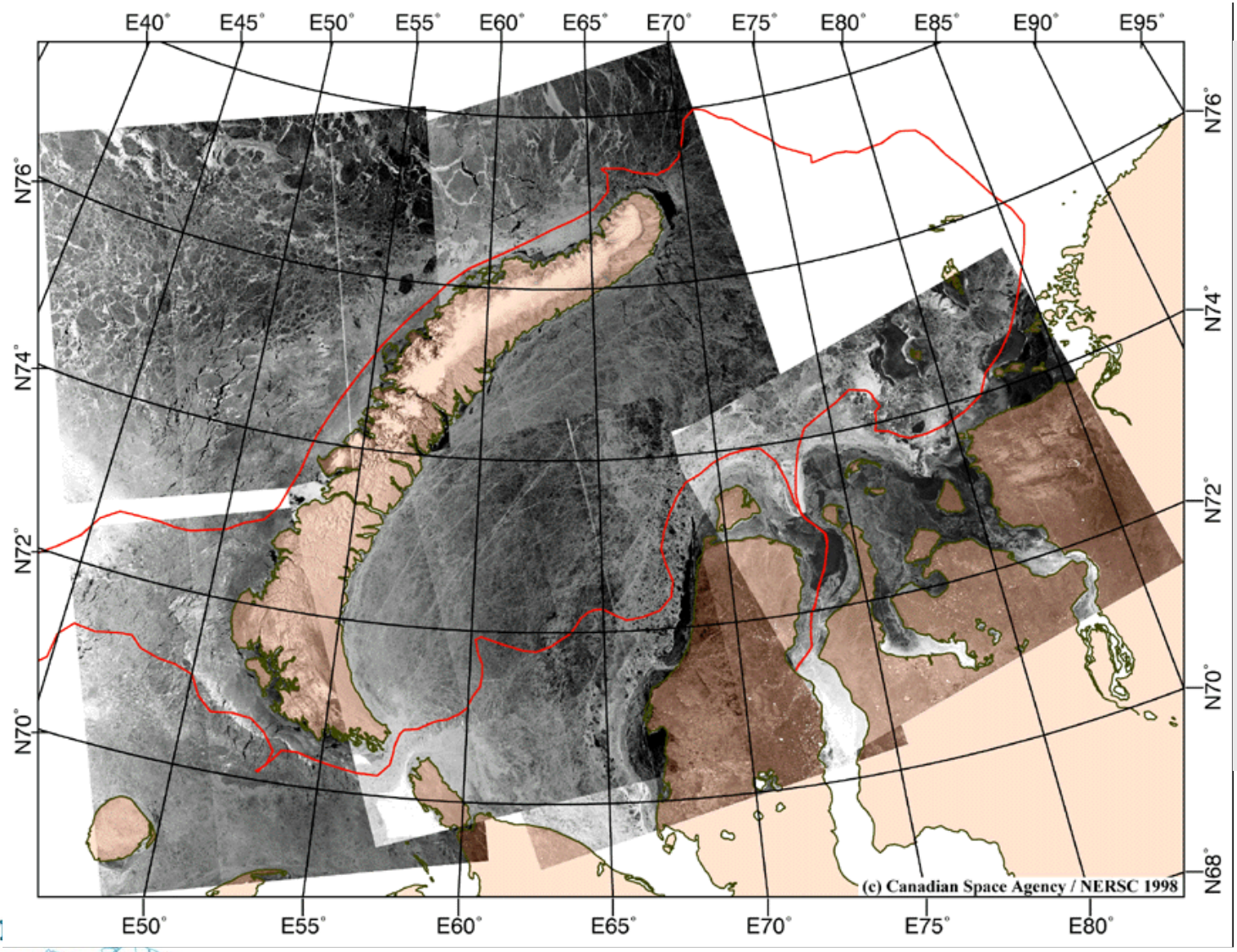

SAR images from RADARSAT were used to plan the optimal sailing route between Murmansk and Ob river.

Due to heavy ice in the Kara Gate, a route to the north of Novaya Zemlya was chosen for the eastbound trip

Breakup of ice shelves in Antarctica

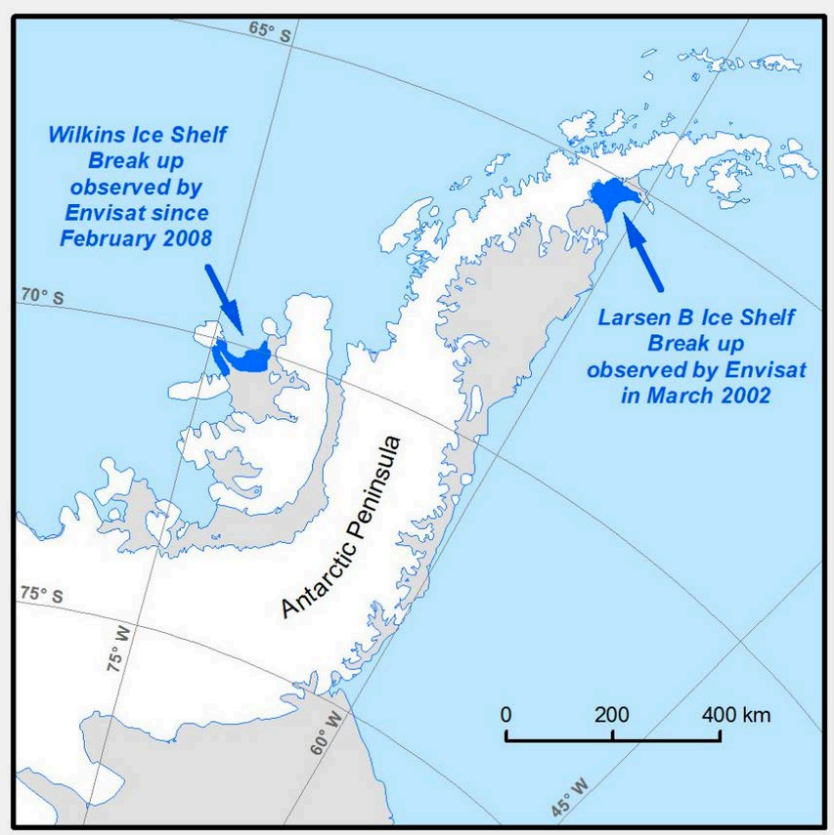

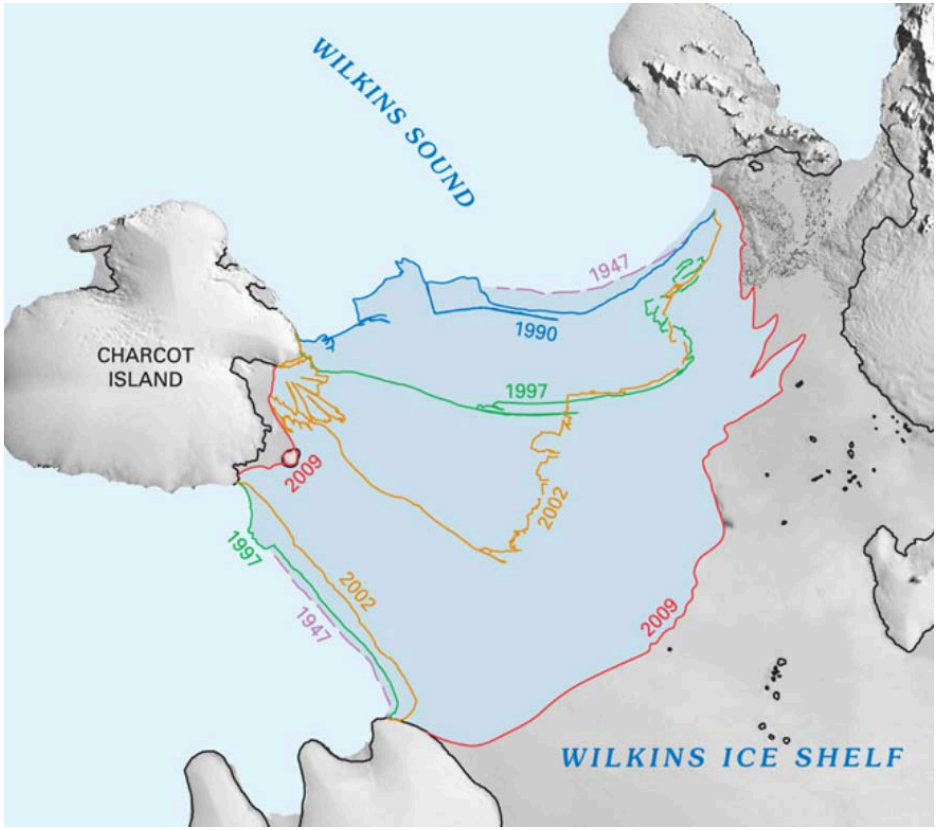

Breakup of Wilkins ice shelf

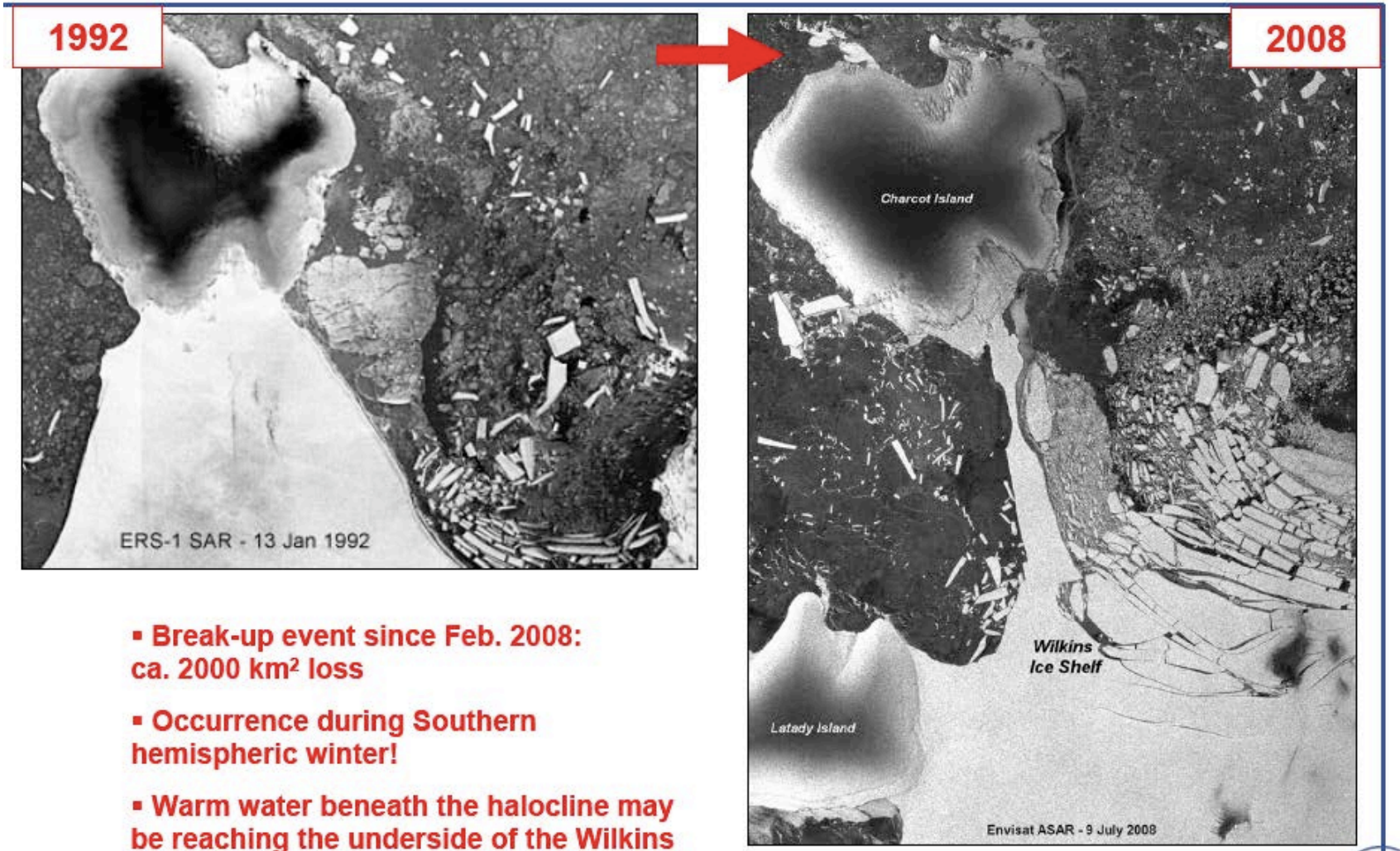

- Break-up event since Feb. 2008: ca. 2000 km² loss
- Occurrence during Southern hemispheric winter!
- Warm water beneath the halocline may be reaching the underside of the Wilkins Ice Shelf and thinning it rapidly

European Space Agency
Agence spatiale européenne

NERSC

the Living Planet

Breakup of Larsen ice shelf

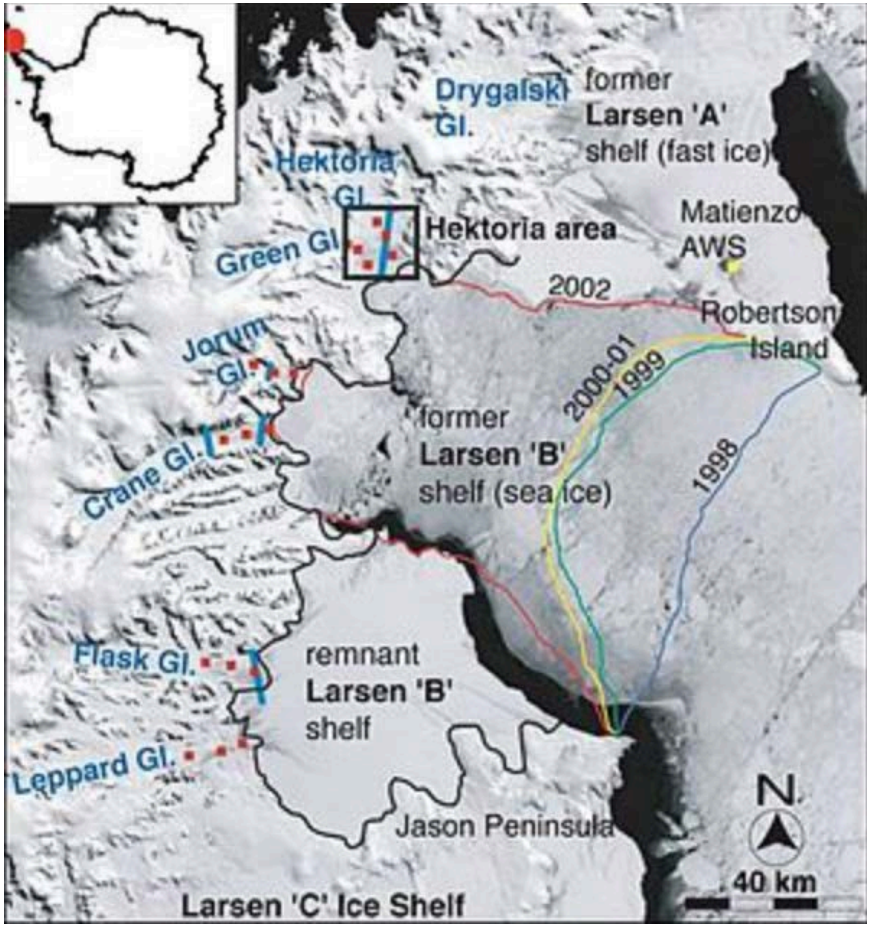

Breakup of Larsen ice shelf – June 2017

Icebergs in Franz Josef Land area: ASAR and TerraSAR-X data

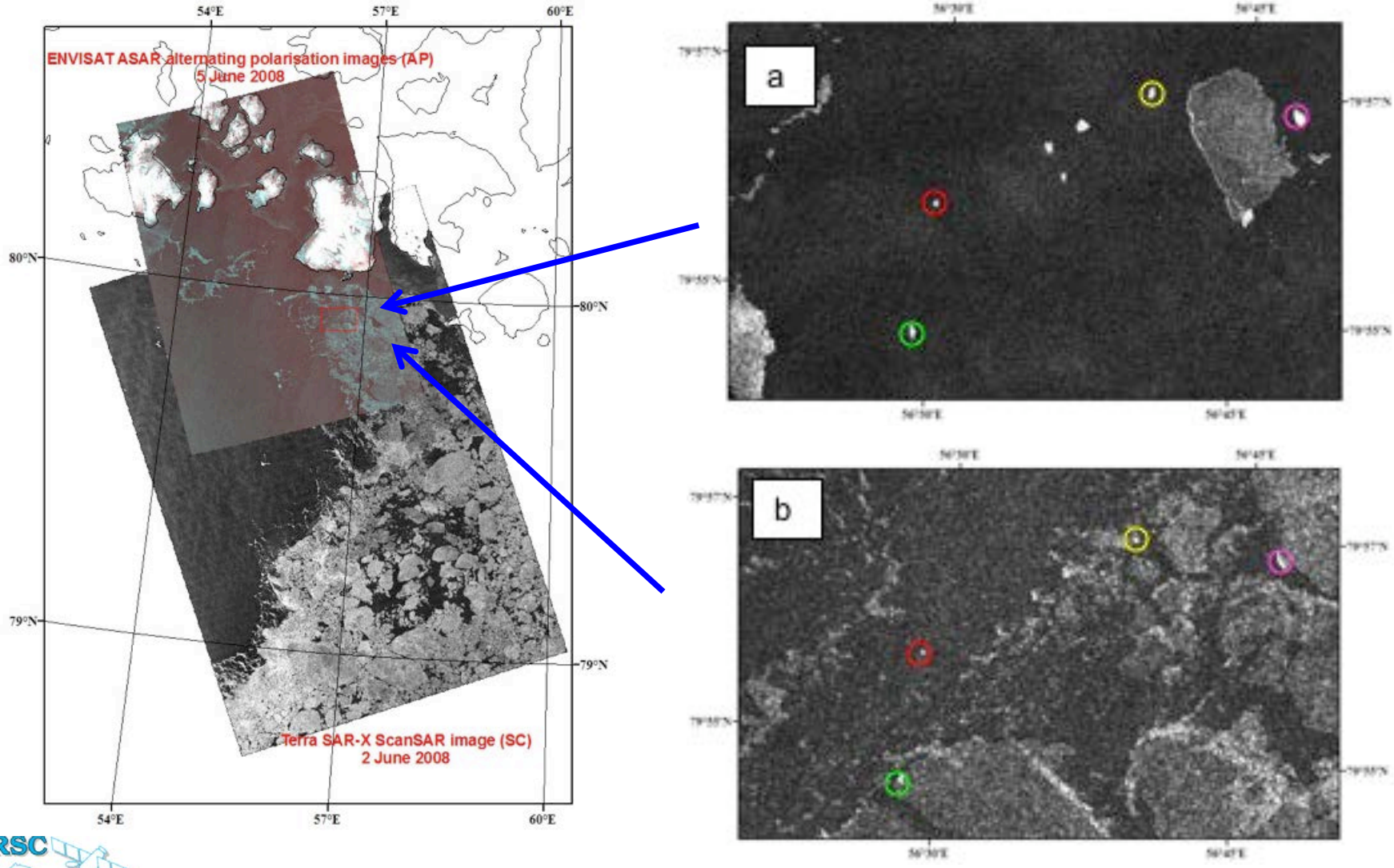

InSAR: Surface topography and movement

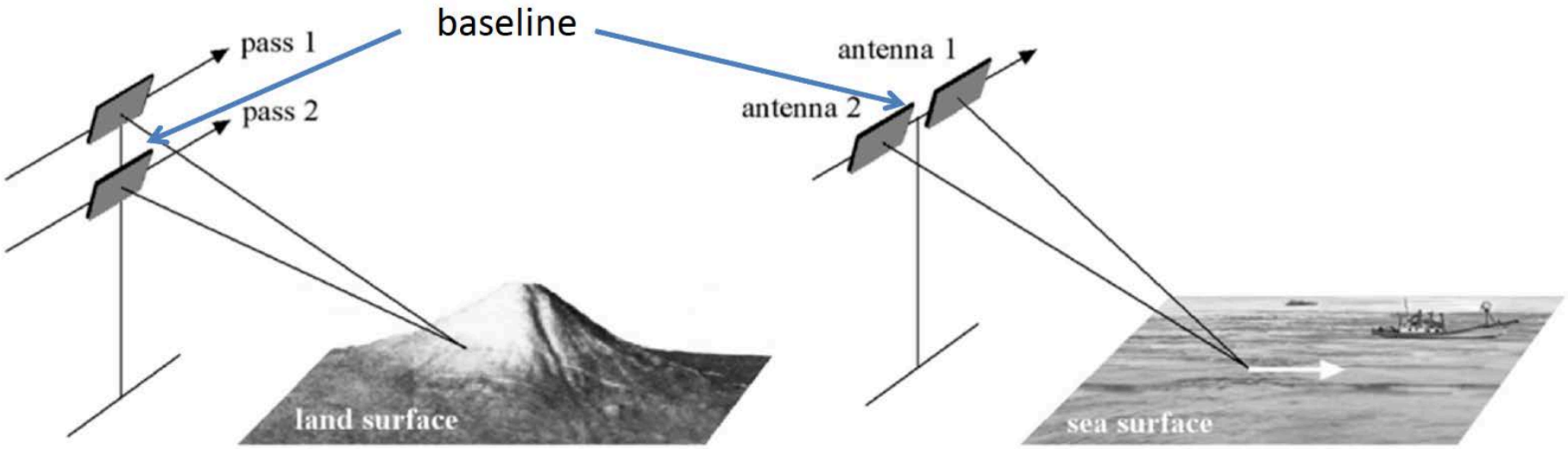

Across-track and along-track interferometry

- sensitive to topography
- not sensitive to motion

- sensitive to movement
- not sensitive to topography

Ref. W. Dierking

InSAR: Sea ice topography, example

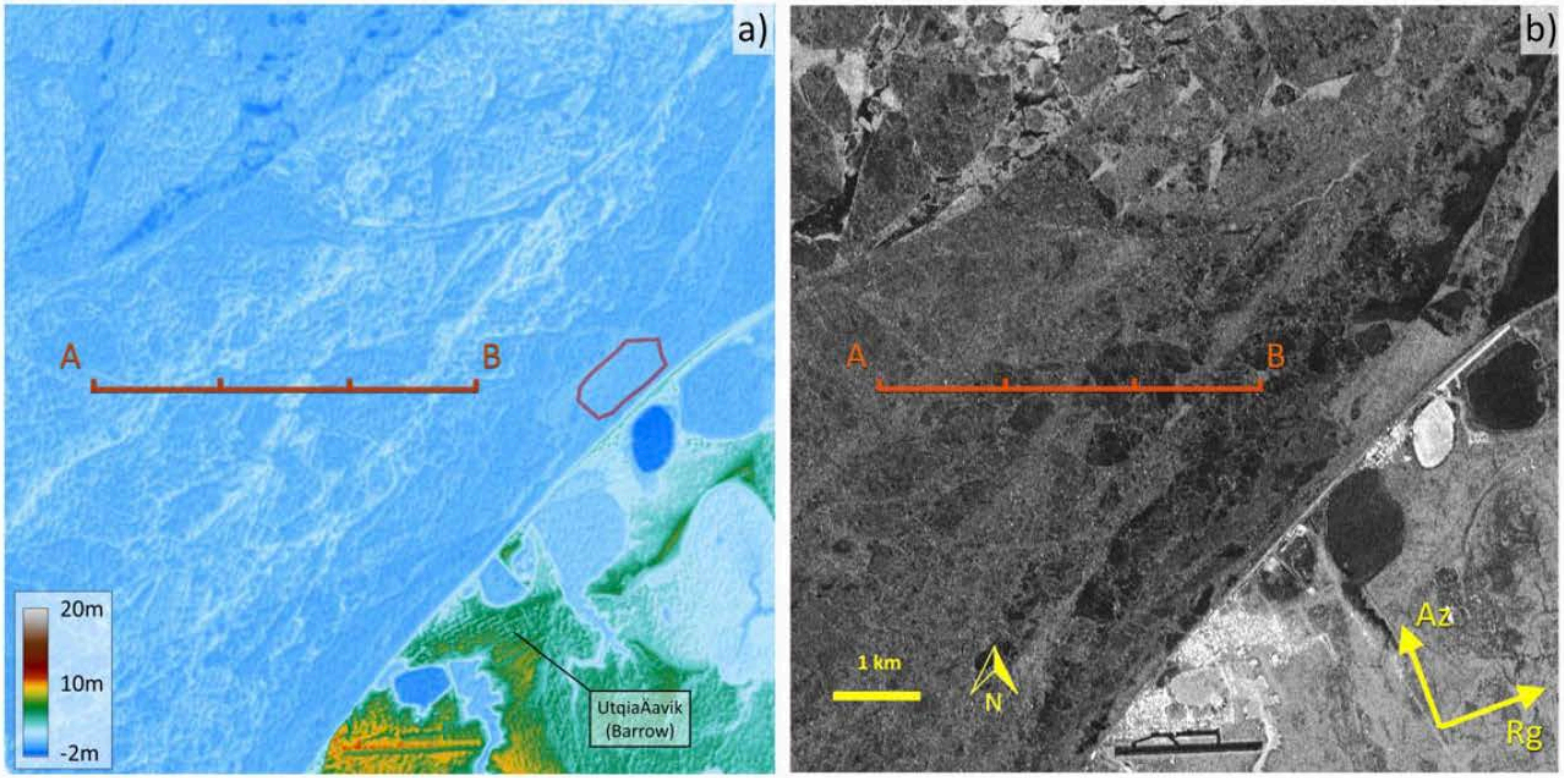

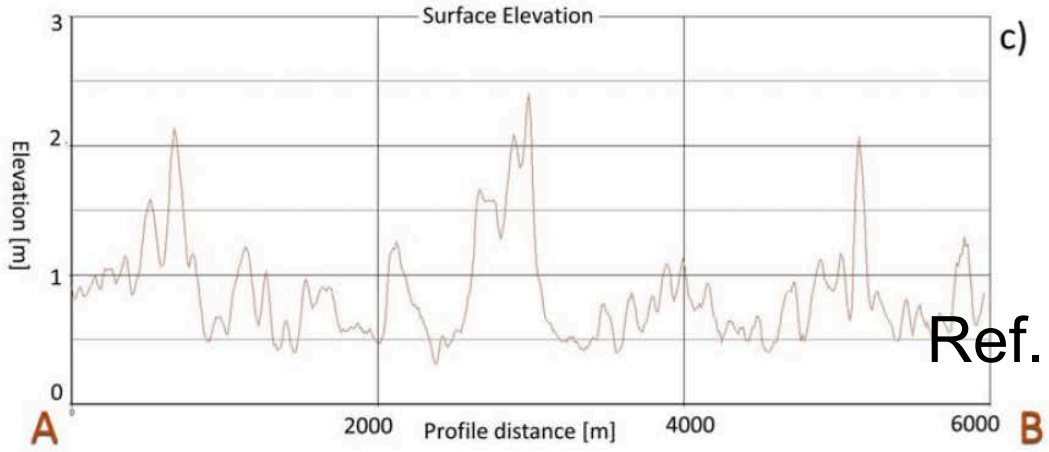

Ref. W. Dierking

InSAR: Topography and Movement

> *Retrieval of topography is possible, but ice drift component perpendicular to the satellite track has to be known to remove the motion phase term: determination of u_{LOS}?*

> *Landfast ice: topographic information needed for trafficability assessments*

> *Case studies only with Tandem-X; satellite constellations (>2) required for operational applications*

Ref. W. Dierking

Evolving use of SAR data for sea ice

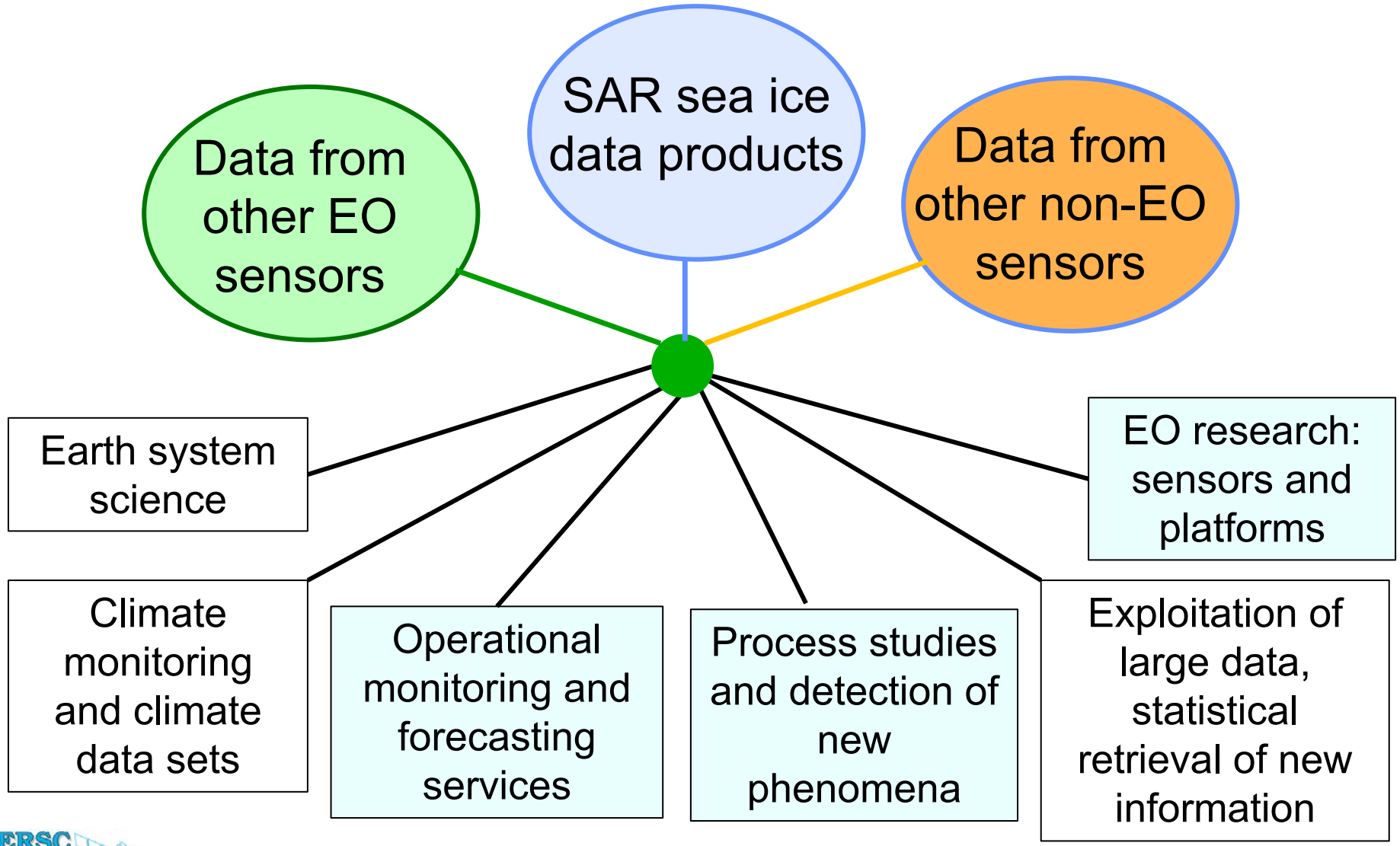

Sea ice is a very changeable medium – will it change more ?

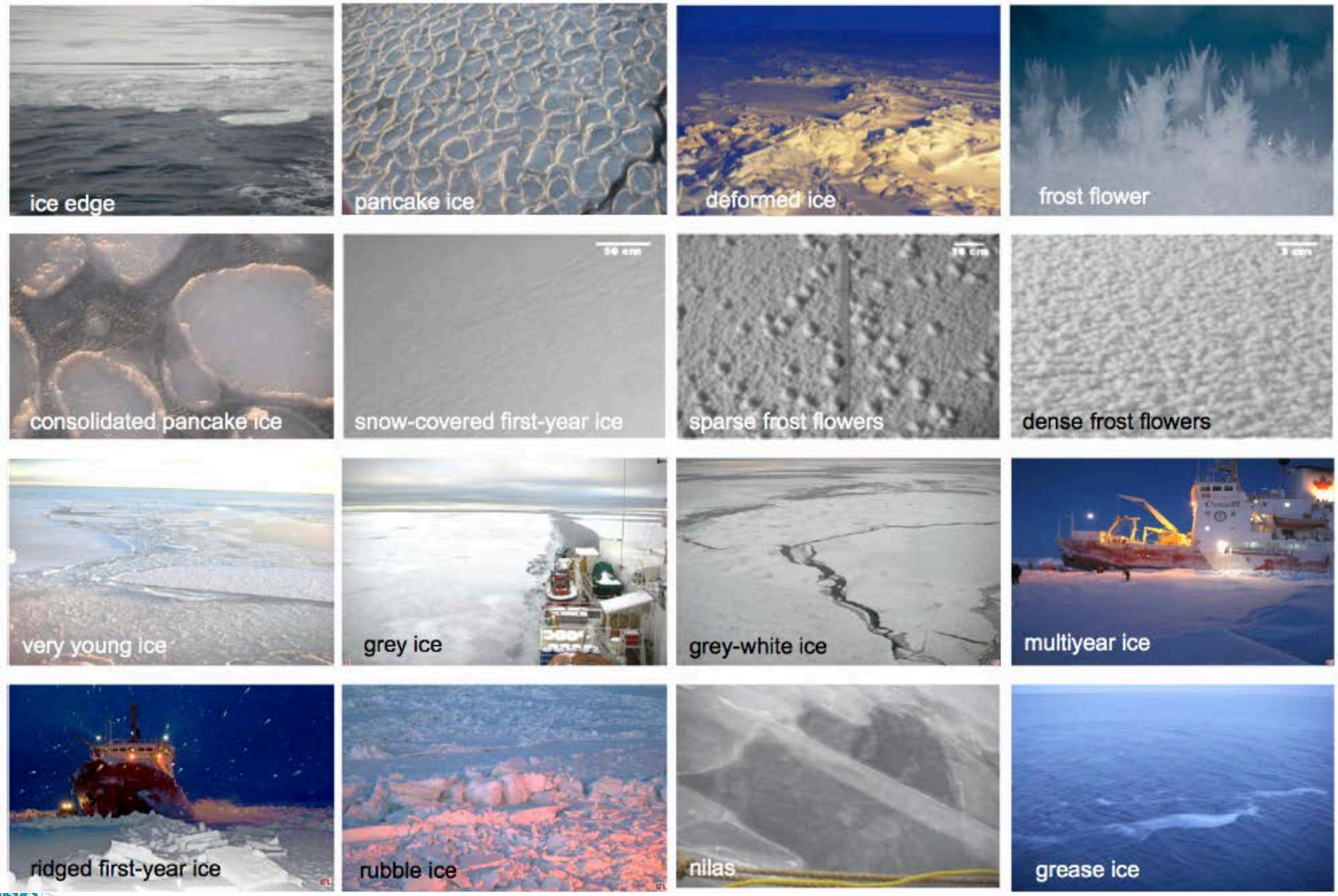

Ref. Gupta, 2014